SPIS 5: new modelling capabilities and method for scientific mission

P. Sarrailh, J.C. Matéo-Vélez, S. Hess, J.F. Roussel, B. Thiébault, J. Forest, B. Jeanty-Ruard, A. Hilgers, D. Rodgers, F. Cipriani

(Abstract No# 209)

SPIS 5: new modelling capabilities and method for scientific mission

Pierre Sarrailh, Jean-Charles Matéo-Vélez, Sébastien Hess, Jean-François Roussel, Benoit Thiébault,

Julien Forest, Benjamin Jeanty-Ruard, Alain Hilgers, David Rodgers, Fabrice Cipriani

***Abstract*— Since the last version, the numerical core and the user interface of SPIS have been significantly improved to achieve two objectives: to make SPIS more user friendly and robust for an industrial use and to extend the multi-scale capabilities and the solvers precision to be usable to model scientific missions. The new numerical algorithm and the new modelling capabilities are presented in detail. It permits to model environment varying conditions, spinning spacecraft, semi transparent grid, secondary emission from 1D thin element (i.e. wires or booms), 2D thin elements (solar arrays for examples), the effect of the E×B field, the particle detector on spacecraft or the Langmuir probes on board.**

Keywords—Plasma, modeling, Particle-In-Cell, numerical method, spacecraft interactions

I. Introduction

Initially released in March 2004 [1], SPIS, the Spacecraft Plasma Interaction Software [2], [3], was developed by ONERA and ARTENUM and is freely available [4]. Since the initial release, the SPIS software has become the European standard for the modelling and the simulation of the spacecraft plasma interactions. A large part of the physical phenomena involving the spacecraft charging was already implemented in the previous version of SPIS (version 4.3). It was used to simulate to model spacecraft interactions with space plasmas [3], [5]–[7] or ground plasmas [8], [9], probe behavior [8], [10], or electric propulsion-induced environment [11]–[13], or LEO drifting plasma [14]. Scientific missions in Solar wind tenuous plasma and extreme experimental conditions were also covered, as reported in [15]–[17].

Since this version, released in 2010, the numerical core and the user interface of SPIS [4] have been significantly improved to achieve two objectives: to make SPIS more user friendly and robust for an industrial applications and to extend the multi-scale capabilities and the solvers precision to be usable to model scientific missions. To address these issues, ESA has initiated the development of a new version of SPIS through two different activities. The first activity called SPIS-GEO was dedicated in a complete refactoring of the SPIS user interface, some improvements of the numerical solver robustness and a validation campaign done in an industrial context (two companion papers have been proposed on this subject). The second activity called SPIS-SCIENCE, with extended models and advanced plasma diagnostics.

This paper presents the efforts in numerical core improvements made to answer the user requirements expressed by the scientific community during the 12th Spacecraft Plasma Interaction Network in Europe (SPINE) meeting [18]. In section II, the modeling requirements in term of precision and performance to simulate the full range of conditions encountered during science missions are presented. The next sections are dedicated to the description of the major improvements of the numerical solvers that are currently used by the SPIS 5 users.

II. Modeling requirements

The main interest of the scientists is to estimate the electrostatic potential effect on the low energy particle or electric field measurements in-flight (illustrated in different companion papers). It requires a robust, accurate and performant simulation of the potential on the whole surfaces of the spacecraft but it also required to assess a very multi-scale problem. For example; the scale ratio between a spacecraft typical length and a particle detector aperture is five orders of magnitudes. Most of the scientific missions requires to models booms or solar arrays. In this section, we will present successively the general approach used for these simulations and the enhancements done in SPIS 5.

A. General approach

The approach of a SPIS simulation consists on an iterative resolution of the electric potential in volume, the particle transport, the particle interactions with the spacecraft and the calculation of the electrical potential on the spacecraft (as represented in Fig. 1). The SPIS numerical core called “SPIS-Num” has been developed in a modular flexible structure (Java Object Oriented [2]). All types of objects under use follow a generic model (typically an abstract class), which allows defining new versions that can be integrated without further work. The numerical core architecture is divided into three levels: the spacecraft level (top level), field-matter coupling level and matter level (down level). The spacecraft level includes the computation of the spacecraft equivalent circuit and the surface interactions. It is responsible of:

P. Sarrailh, J.-C. Matéo-Vélez, S. Hess and J.-F. Roussel are with Onera – The French Aerospace Lab, Toulouse, France (e-mail: pierre.sarrailh@onera.fr)

B. Thiébault, J. Forest, B. Jeanty-Ruard are with Artenum, Paris, France

A. Hilgers , D. Rodgers, F. Cipriani are with European Space Agency, ESTEC, Noordwijk, The Netherlands

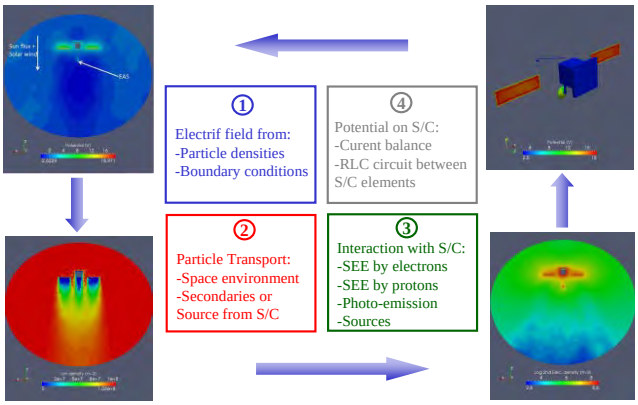

Fig. 1. Principle of SPIS 5 (and older versions) simulations – with an example of a S/C in solar wind.

- Computation of the collected current
- Computation of the emitted current (sources, interactions)
- Surface potential evolution are computed with the circuit solver (conductance, capacitance and inductance model)

The field-matter level is composed by the field solvers and the volume interactions. It is responsible of:

- Poisson equation calculation
- Computation of the interactions in volume (Elastic collision, charge exchange, …)

The matter dynamic level that is responsible of the transport of the particles resolving fluid equations (Maxwell-Boltzmann) or using a Particle-In-Cell or a backtracking approach.

The evolution of the potentials on the spacecraft involves an equivalent circuit taking into account the coating capacitances and conductance (surface and volume conductivities), and also user-defined "discrete" components (extra resistors, biases or capacitors added between subsystems). A spacecraft circuit implicit solver was designed to handle problems with very different time scales thanks to physics predictors of the plasma current variations in reaction to potential changes.

Surface interactions between the plasma (primary or secondary) and the spacecraft considered in SPIS are the secondary electron emission under electron and photon impact. Yields are calculated automatically within SPIS pending on macroscopic material properties defined at user level. For instance the yield of true electron emission under electron impact is computed using the maximal yield and the energy of the maximum. Distribution functions are Maxwellian in volume (or Lambertian in surface). Secondaries from secondaries are activated for electrons from environment and artificial sources on spacecraft. Artificial sources models are maxwellian (possibly with a drift), axisymmetric and two axis symmetry (plus sources like field effect emission). Erosion model is applicable to Xenon ions.

Concerning fields, the Poisson equation finite element solver follows a pre-conditioned conjugate gradient method. The boundary conditions can either be Dirichlet, Neumann or a mix of them (known as Robin or Fourier), which allows a better modelling of pre-sheath conditions (1/rn behaviour). Non linear Poisson equation (i.e. Poisson including Boltzmann distributions for the electrons) can also be solved with an implicit method, offering stability even for a Debye length smaller than cells. Specific features were added to handle singular geometries, either very thin wires (of which radius cannot be meshed without generating degenerated elements) or very thin plates (of which edges cannot be meshed). The method consists in analytically subtracting the singular part of the potential field resulting from the geometrical singularity, and solving the regular part (this splitting being of course transparent for the user).

Concerning matter, the main models are a Particle-In-Cell (PIC) solver for a Monte Carlo solving of Vlasov equation, and a Boltzmann distribution to describe the thermal equilibrium distribution of electrons. Particle source distributions include a whole library. Gas phase collisions can be modelled through a MCC method, with only charge exchange reactions implemented as of today. A complex 3D multizone model was defined to handle simultaneously in a single simulation a dense quasi neutral region and a space charge region, typically influenced by an unscreened positive potential nearby.

The time scheme represented in Fig. 2 is formed by three integration loops imbricated. It permits to adapt the time steps and the integration duration at each level and for each matter population.

B. *Enhancement in the SPIS 5 version*

The 17th SPINE meeting [18] has been organized in the frame of SPIS-SCIENCE project. It has consisted on a workshop on electrostatic cleanliness effects on the measurement of low energy plasma and electric fields during scientific mission. The SPINE community has permitted to extract the higher priority SPIS modeling requirements that are the followings:

- Numerical instruments modules aiming at measuring particle spectrograms and plasma characteristics within the course of the simulations
- Semi-Transparent Grids to mimic scientific

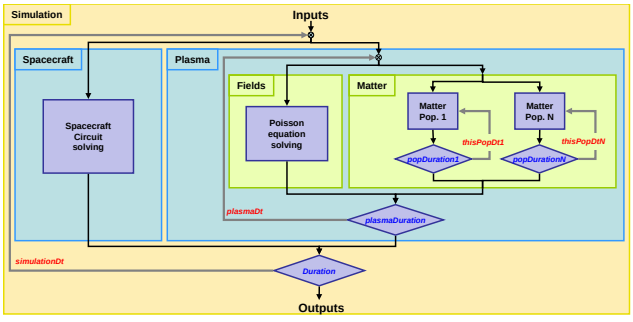

Fig. 2. Time integration scheme of SPIS 5.

instrumentation.

- Non-maxwellian distribution functions for ambient an secondary populations
- Thin elements such as wires and solar panels
- Performance and accuracy increase
- Extension of material properties
- Development of Transitions aiming at simulating transient phase in some typical situations.

The SPIS 5 version has permitted to answer to most of these requirements. The detail of the most important developments is presented in the next sections.

III. PHYSICAL MODELS IMPROVEMENTS

A. *Unlimited population number*

In the previous version of SPIS, the environment populations were limited to Bi-Maxwellian populations for ions and electrons. In the current version, the number of population to model the environment is no longer limited in number and in distribution type (non-Maxwellian distribution function described in section C).

B. *Boundary conditions*

Boundary conditions are a crucial aspect of plasma simulation and a good set of boundary conditions is very important for precise plasma and spacecraft charging diagnostics. In Spis 5, they have been upgraded in several ways.

First, the boundary condition for the electric field can be automatically changed between a pre-sheath model (1/r2 decrease of the potential) and a vacuum-like model (1/r) depending on the local potential on the boundary and on the plasma temperature. It automatically shifts locally to a pre-sheath model if the external boundary is locally outside the sheath, and inversely. Of course, it is still possible for the user to set fixed boundary conditions (including Fourier, Neumann or Dirichlet conditions), as in previous code versions.

Second, the injection of Maxwellian populations at the external boundary has been significantly improved by adjusting both the flux and the distribution function of emitted particles as a function of the local potential. The objective was to keep a good precision while the plasma sheath extends outside the simulation box. We have made the assumption of an OML regime in case of attractive potential and of a Maxwell-Boltzmann regime otherwise. The surface flux of repulsed specie is given by the Boltzmann theory:

$$F_{repulsed} = n_0 \sqrt{\frac{eT}{2\pi m}} \times \exp(\chi) \tag{1}$$

$$\text{with } \chi = -\frac{q}{e}\frac{V}{T} \tag{2}$$

where q is the particle electric charge, e the elementary electric charge, T the energy expressed in volt unit, n0 the density in undisturbed plasma and m the mass. SPIS permits to perform injection assuming 2D or 3D geometries. The flux of the attracted specie is given by the OML theory. In 3D spherical geometry it writes:

$$F_{OML,3D} = n_0 \sqrt{\frac{eT}{2\pi m}} \times [1+\chi] \tag{3}$$

In 2D cylindrical geometry it writes:

$$F_{OML,2D} = \frac{2}{\sqrt{\pi}} \times n_0 \sqrt{\frac{eT}{2\pi m}} \times \left[\sqrt{\chi} + \frac{\sqrt{\pi}}{2} \exp(\chi)\, \mathrm{erfc}\left(\sqrt{\chi}\right) \right] \tag{4}$$

Liouville's theorem states the distribution function is constant along a particle trajectory. In 3D, the isotropic velocity distribution function is:

$$f(\mathrm{v}).d\mathrm{v}_T = \begin{cases} \dfrac{m\mathrm{v}^2}{2eT} > \chi, n_0 \times 4\pi \exp(\chi) \times \left(\dfrac{m}{2\pi eT}\right)^{3/2} \mathrm{v}^2 \\ \qquad \times \exp\left(-\dfrac{m(\mathrm{v}^2)}{2eT}\right) d\mathrm{v} \\ \dfrac{m\mathrm{v}^2}{2eT} > \chi, 0 \end{cases} \tag{5}$$

In 2D coordinates, assuming a cylindrical symmetry of potential and no time dependence, the distribution function injected writes:

$$f(\mathrm{v}_r, \theta, \mathrm{v}_z).d\mathrm{v}_T = \begin{cases} \dfrac{m\mathrm{v}_r^{\,2}}{2eT} > \chi, n_0 \exp(\chi) \times \left(\dfrac{m}{2\pi eT}\right)^{3/2} \mathrm{v}_r \\ \qquad \times \exp\left(-\dfrac{m(\mathrm{v}_r^{\,2} + \mathrm{v}_z^{\,2})}{2eT}\right) d\mathrm{v}_r\, d\theta\, d\mathrm{v}_z \\ \dfrac{m\mathrm{v}_r^{\,2}}{2eT} > \chi, 0 \end{cases} \tag{6}$$

C. *Non-Maxwellian distribution functions*

A new set of velocity distribution functions has been developed to increase the previous code capabilities, which only supported Maxwellian distributions for ambient particles (possibly drifting for ions). Distribution functions (DF) of PIC populations are passed or transformed internally in tabulated DF. The most general case is a DF defined versus three velocity components, basically in a Cartesian coordinates system, but also possibly in polar coordinates. As a result any kind of DF can be represented.

In the natural space environment, plasma are generally observed to possess non-Maxwellian high energy tails. A useful distribution to model such plasma is the isotropic kappa distribution:

$$f_\kappa(v) = \frac{N}{\pi^{3/2}} \frac{1}{\theta^3} \frac{\Gamma(\kappa+1)}{\kappa^{3/2}\Gamma(\kappa-1/2)} \left(1 + \frac{v^2}{\kappa\theta^2}\right)^{-(\kappa+1)} \tag{7}$$

$$\theta = \left[(2\kappa-3)/\kappa\right]^{1/2} (kT/m)^{1/2}$$

The transformation of an isotropic kappa distribution into a tabulated distribution function has been implemented. The same work has been performed for Maxwellian distributions (possibly with a drift).

Thanks to the genericity of SPIS code, tabulated distributions functions can be defined for any population, including particles coming from the spacecraft. In this case however, only isotropic distributions are permitted.

The injection of generic 3V DF can be very costly in term of computational duration. The capability to define isotropic tabulated DF has been offered to users, which reduce significantly the computational cost.

D. Transitions

Transitions consist in the modification of parameters within the course of the simulation. The change of these parameters is defined during the pre-processing phase through ASCII tables and the simulation automatically applies the changes without extra operation of user. In the future, it could be envisaged however that the user defines a transition in real-time, i.e. interfering directly with a running simulation. Several transitions are available: eclipse exit, spinning spacecraft, artificial source (de)activation. The eclipse exit scenario is particularly useful to estimate the ESD risk on GEO spacecraft. Dielectrics can attain huge differential charging during eclipse, due to low temperature dielectrics resulting in high resistivity. At eclipse exit, ESDs triggered at solar cell level due to the eclipse charging phase charge may lead to secondary arcing powered by solar arrays. The spinning spacecraft transition is defined by a spin axis and angular velocity. The sun flux and particle injection at external boundaries is automatically updated in time. It aims at simulating the configurations when charging time scale is comparable to the spin velocity. In such cases, the charging dynamics at a given time may significantly differ from the steady-state regime obtained for the corresponding frozen spacecraft attitude. Finally, the artificial source transition regime permits to define a time variation of each artificial source defined on the spacecraft. Possible example may consist in activating a plasma thruster, an electron gun or modelling the sudden injection of plasma generated by a micrometeoroid impact.

Thanks to the genericity of SPIS, the range of possible transitions is unlimited, and it is possible to set several transitions during a simulation.

E. V cross B field

In some cases, the magnetically-induced electric field, i.e. generated by the motion of the spacecraft in a magnetic field, can lead to voltage drops of tens of volts on large spacecraft conductive elements.

Poisson equation is solved in the referential R of the plasma to provide the volume electric potential ϕ. The external boundary conditions are unchanged with respect to past SPIS implementations. The boundary conditions on the spacecraft surface are changed to fit the Hall effect: the Dirichlet potential ϕ is calculated on each point of coordinates x of the spacecraft surface using the potentials ϕ' in the referential of the spacecraft *R'*:

$$\phi = \phi' + (\mathbf{V_{SC}} \otimes \mathbf{B}) \cdot x \tag{8}$$

where VSC is the spacecraft velocity. ϕ is defined to an arbitrary constant depending on the reference position x0 leading to $\phi = \phi'$. It was decided to set x0 such as:

$$\max[(\mathbf{V_{SC}} \otimes \mathbf{B}) \cdot x] = 0 \tag{9}$$

The strong advantage of solving the Poisson equation in plasma referential is that, in the case where a Maxwell-Boltzmann distribution can be assumed for electrons in the referential at rest, the formulation used in SPIS (for density and in the Poisson non-linear solver) remains unchanged since such species are in equilibrium with ϕ and with not ϕ'. The particle dynamics is solved in the referential R' of the spacecraft since their positions x', velocity v' (and current collection/emission on spacecraft) were all defined in the reference frame of the spacecraft mesh. The particle pusher solves the equation of the dynamics in R':

$$\dot{x}' = v' \tag{10}$$

$$\dot{v}' = \frac{q}{m}(E + v' \otimes B + V_{SC} \otimes B) \tag{11}$$

IV. THIN ELEMENTS

A. Thin wires

Modeling conductors with very small radius compared to the typical dimension of the spacecraft makes the calculation cost high or even impossible in most of the cases. The meshing requirement implies that the mesh refinement should be smaller that the wire radius to describe the wire geometry. Furthermore, if the Poisson equation is taken into account, a mesh refinement well smaller than the wire radius is required:

$$dx < rad / 5 \tag{12}$$

The idea is to not have to mesh this element considering that the wire is represented by 1D elements of mesh (i.e. mesh edges). But simply imposing a Dirichlet condition on this

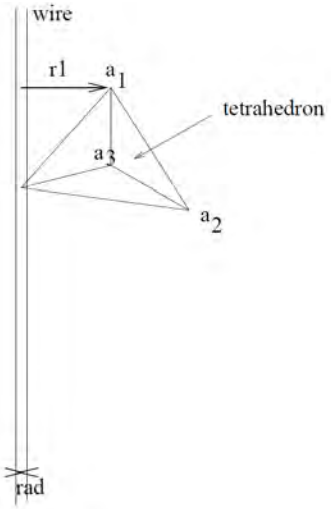

Fig. 3. Schematic representaion of th thin wire approwimation

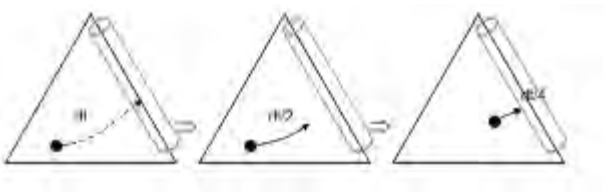

Fig. 4. Dichotomie method for particle collection on the wire elements

edges is not sufficient, a more advanced boundary condition is needed to model the potential evolution in the surrounding cell to mimic a wire element [19]:

$$\frac{\partial u}{\partial n}(a_i) + \frac{u(a_i)}{r_i \ln(r_i/rad)} = \frac{r}{r_i \ln(r_i/rad)} \quad (13)$$

Where r_i is the distance from the closest node i to the wire and *rad* is the radius of the wire (see Fig. 3). As this approximation mimics a 1D wire approximation, it should be used when the wire length is well greater than the radius and when the mesh element refinement is well larger than the radius:

$$dx > 5 \times rad \quad (14)$$

The limitations of this kind of approach come from the fact the elements size of the mesh has to be sufficiently large. It requires that the singularity created by the wire potential is mostly inside the cells in contact with the wire. It permits to have a solution sufficiently homogeneous in the cells which are not directly in contact with the wire (which compatible with finite elements method). Another limitation comes from the end effects of the wire. There is no model on the singularity created by the ends of the wire which is much more singular. This wire model should be used when the end effect is a sufficient low to be neglected..

Concerning the particle interactions with the wire, the collections, the surface interactions and the effect on trajectory are taken into account. Concerning the trajectories of particles, due to the singularity of potential, the potential cannot be considered to be linear in the cells surrounding a wire. Thus the exact method (supposing no magnetic field and linear potential in each cells) implemented in SPIS can not longer be used in this case. A Runge-Kutta method (order 4 and 5) is thus used to compute the trajectories of the particles. In addition a dichotomy method (see Fig. 4) is used to compute the exact position and angle of collection of the particle on the wire surface (not meshed). The calculation of the interactions of the particle with wire takes into account the position of collection and the incidence angle of collection. The direction of emission (as e.g. the secondaries or the backscattered) is isotropic on the wire and does not depend on the collection position around the wire.

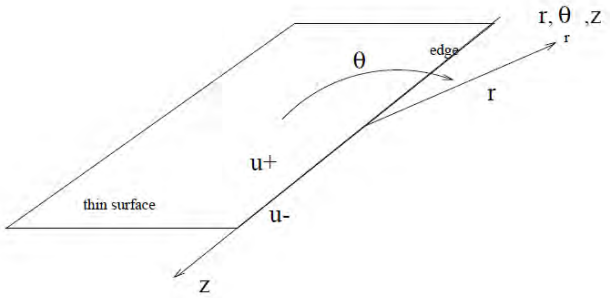

Fig. 5. Polar coordinate sytem arround a thin panel edge

B. Thin panels

A frequent example of thin panel is when a solar array is defined in a simulation. The same problem as for a wire element appears. The solar array thickness is most of the time very small in comparison to the other lengths of the panel. A standards calculation would also require having a mesh refinement smaller than the panel thickness. This can be very costly in term of mesh elements and thus in CPU time and memory. This singularity is furthermore very critical as there is most of the time a discontinuity of potential between the top and the rear of the panel. A basis idea is to neglect the thickness in order to not have to mesh the border of the panel. But this situation creates a geometrical singularity on the edges of the panel. The singularity of the geometry and the discontinuity of the potential have to be treated to be solved by the Poisson solver.

In SPIS, this kind of thin elements can be generated at the UI interface by generation a flat 2D panel in the CAD model. In a second step, the Penelope library of SPIS-UI will permit to do a mesh splitting of the mesh elements to obtain a face A and a face B (see Fig. 7 – also used for STG). As the mesh nodes on face A are strictly different from the nodes on face B, this permits to model a strict discontinuity on the edges of the thin element. But this discontinuity and the singularity have to be taken into account in the Poisson Solver. The idea is to make a decomposition of the Poisson equation solution in a singular part and a regular part in order to extract the discontinuous part in the finite element Poisson solver.

$$u = u_{reg} + u_{\sin g} \quad (15)$$

The singular part of the solution is chosen to mimic an edge of an infinite panel with a zero thickness with a potential u+ on the top and u- on the rear (see Fig. 5). In this case, the homogeneous solution will be:

$$u_{\sin g} = (u_- - u_+)\frac{\theta}{2\pi} + u_+ \quad (16)$$

The Poisson equation is then updated to solve the regular solution supposing the singular one.

The major limitation of this approximation is that the mesh refinement has to be greater than the panel thickness but it has also to be smaller than the typical length of the phenomena you have to model. It can be critical in case of dense plasma (small Debye length) or when the geometry imposed high potential gradient on the panel surface.

C. Semin Transparent grid

Semi-transparent grids (STG) are thin spacecraft surfaces bounded by two plasma volumes (see Fig. 6). They collect only a fraction of particles passing through them. They can emit

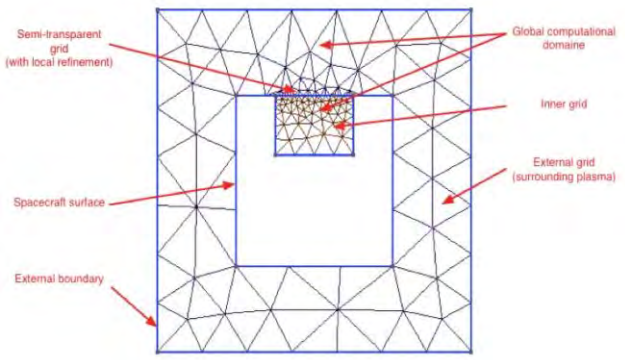

Fig. 6. Example of Cad modelling of a STG inside the computational domain.

secondary particles (from electron, proton and photon impact). This surface mesh is composed of two sides. Side A is the duplicate of face B (see Fig. 7) but with surface meshes oriented in the opposite direction. Side A et side B are concatenated in order to form a single surface mesh.

The grid transparency is taken into account by all particle volume distributions (PIC, Backtracking and Composite). A particle reaching the grid has a probability to pass through the STG corresponding to the transparency. The transparency is treated statistically. When a particle is collected, the particle is added to the surface distribution function living on the STG. When a particle is not collected, the particle continues its trajectory without any modification.

SPIS solvers make the difference between the particles collected on the face A and on the face B. It ensures a correct computation of secondary populations on the both sides of the STG (especially in the case of photoemission where the collected population is photon and the emission is present only on one face of the grid). The transparency is also taken into account for photons: transparency shading effect of photoemission is modelled. The emission of secondary populations is activated with the same flag as on the SC. A STG can support: photoemission, secondary emission by electron impact, secondary emission by proton impact and hoping effect.

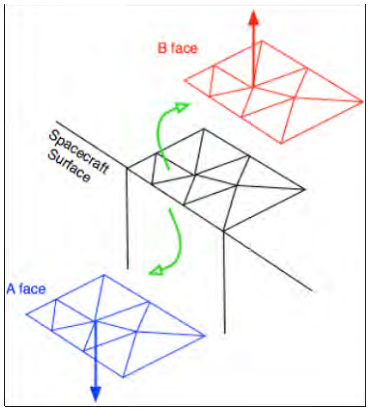

Fig. 7. Design of the surface meshes associated to a STG

The limitation of this approach comes from the fact the meniscus effect on the electrical potential is not taken into account. On a real grid, if the grid is placed in a region where a potential gradient exist, the potential at the center of the apertures of the grid can be smaller of higher than the potential on the grid. This phenomenon depends on the external conditions around the grid and on the grid geometry. If the grid holes are smaller than the grid thickness or when the holes are well smaller than distance between holes or if the hole radius is small in comparison to the external potential gradient typical length, the meniscus effect can be negligible and the approximation done in SPIS is good. Otherwise, two phenomena can appear: A deflection of particle passing through the grid or a transparency factor depending on the particle energy. These phenomena are not modelled in SPIS when the user chooses the STG model. In this case that they are not negligible, the user has to model the detailed geometry of the grid (meshing the holes).

D. Solar array interactor

The development of "Solar arrays plasma interaction concerns the effect of small metallic units set to high voltages, as e.g. interconnectors of a solar array. The solar arrays modelling is quite complex since they are composed of a series of solar cells assembly, basically a solar cell with a cover glass. At a first order of approximation, it can be interpreted as a large surface of dielectric covering. However, in some case, especially in LEO or in the solar wind, the current collection by the metallic interconnects can largely contribute to the global spacecraft charging. The model implemented in Spis 5 assumes no change in the geometrical model (no mesh refinement). The user can define the ratio of a surface area which is metallic, a collection law and the bias voltage of the circuit behind the dielectric (with respect to spacecraft ground). The fraction of the current collected by the dielectrics and attributed to the interconnects follows a collection law (as e.g. OML assumption). It aims at modelling them not at the length scale of the panel and not at the length scale of the interconnectors (not meshed – see Fig. 8). At this scale, we can make the assumption that the solar array surfaces are dielectric surfaces, through which a part of current is collected directly by the ground, i.e. not by the dielectric surfaces of the solar cell. The electric field is also disturbed at the vicinity of these highly biased small elements. The interconnector modelling is based on the following assumptions:

- The solar array mesh need not being adapted to the interconnects size

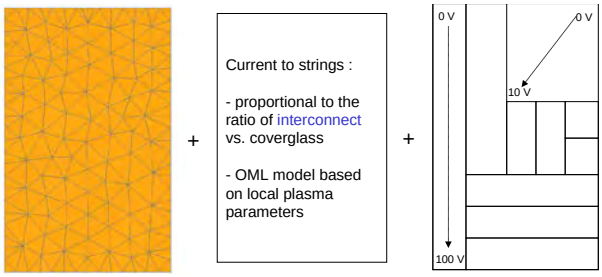

Fig. 8. Schematical view of the interconnector modelling

- The current collection on the solar array is calculated as a standard simulation, i.e. the plasma is not globally affected by the interconnect
- Locally in each cell of the solar array, the current is distributed between the cover-glasses and the interconnects
- The current distribution is affected by the potential of the interconnects behind the cover-glasses (map defined by the user).

The ratio of current collection is defined as a function of the reduced differential potential and a geometrical factor. The differential potential is defined as the difference between the potential at the dielectric surface and the potential of the electrical node of the solar array. Then, the reduced differential potential is the ratio between the differential potential and the particles energy in [eV]. When the current ratio is defined in a file, the both effects are supposed to be taken into account within the file. By default, when no file is defined, a cylindrical OML like law is used. The probability for a particle to be collected is:

$$proba = \frac{R \times \sqrt{1 + V_{diff,reduced}}}{(1-R) + R \times \sqrt{1 + V_{diff,reduced}}} \quad (17)$$

Where R is the geometric ratio defined by the user and Vdiff is the reduced differential potential.

V. Numerical Instruments

The possibility to monitor ambient or artificial populations with a high level of information is provided in SPIS 5 by the way of numerical Instruments. Three types of numerical instruments are defined in SPIS: the Plasma Sensors, the Particle Detectors and the Virtual Particle Detectors. The ParticleDetector provides mainly the particle distribution functions on dedicated spacecraft surfaces. They basically rely on a Test Particle (TP) method which consists in calculating the particle trajectories in a frozen electromagnetic field, by a series of forward and backward tracking. The LangmuirProbe instrument extends the ParticleDetector class by introducing IV sweep coupled with TP. The VirtualParticleDetector has basically the same architecture except it performs the TP onto surfaces outside the spacecraft (virtual surfaces). They do not interact with the plasma and spacecraft dynamics. The PlasmaSensor class provides regularly the time evolution of scalars (or more complex data such as distribution functions or linear data) in the plasma volume domain during the simulation (such as potential, density). It is mainly used to check the convergence of the plasma dynamics at a specific location of the plasma volume (not on the spacecraft). They do not interact with the plasma and spacecraft dynamics.

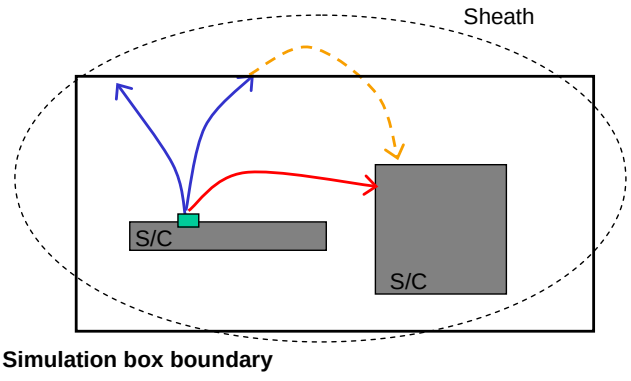

Fig. 9. Backtracking principle from a detector

A. Plasma sensors

Plasma sensors permit to follow the evolution of plasma parameters, at given points of the plasma volume. It concerns the plasma potential, plasma population density, energy and distribution function. More complex instruments provide flux distribution function on spacecraft elements, in order to mimic the measurements performed by particle detectors. A test particle method is used to increase the statistics of particle collection on very small particle detectors, compared to spacecraft dimensions. Last, instruments will also consist in generating such results on a virtual surface mesh, i.e. independent of the simulation domain.

B. Particle detectors

The Particle Detectors instruments in SPIS have been developped in order to address the multiscale proble of the real instruments onboard of spacecraft. As represented on Fig. 9, a backtracking technique permits to track the primary and secondary particles from a real or a virtual surface to the apertures of a real detector. The use of a reverse trajectory method, so-called backtracking, in which electrons is followed from the detector surface, simply reversing time. When the trajectory reaches the plasma domain external boundary (located far from the object), it is assumed as an ambient electron trajectory. When it reaches the spacecraft, it is counted as a secondary electron. Using the Liouville's theorem provide the particle numerical weight (number of real particles represented by the numerical particle). The advantage of the backtracking is getting a better statistics on electron collection, since the classical forward tracking leads to diminish the number of numerical particles by cell when getting close to the object which has a better grid refinement (injected particles are moved towards regions of larger cell number density, hence they spare between more cells). The algorithm also relies on an OcTree method, permitting to refine smoothly the three-velocity distribution function. It permits to obtain data on the relevant energy domains

C. Backtracking algorithm

The backtracking technique is based on the Liouville theorem that states the distribution function value is constant along a particle trajectory. Thus, an exact calculation of the distribution function on the detector implies to compute infinity of trajectory for all the velocities of a velocity range. As it is not possible, the principle is to discretize the velocity space on the detector in velocity volume element $(dv_x. dv_y. dv_z)$. A velocity volume element is a slab between (v_x, v_y, v_z) and $(v_x+dv_x, v_y+dv_y, v_z+dv_z)$. In each volume element (slab), the value of the distribution function is unique. Sometimes in backtracking codes, the value of a distribution function in the velocity volume element is computed at the center of the element. The test particle has an initial velocity of $(v_x+dv_x/2,$

$v_y+dv_y/2$, $v_z+dv_z/2)$. Or it could be computed at the corner of the volume element. These methods are quite efficient for very regular distribution function but fail in the general cases. For example, this determinist method fails when there is a strong selection in energy by the detector. In SPIS, a Monte Carlo technique is implemented.

In each velocity volume elements, a certain number of test particles are created (defined by the user – on the order of 10). For each test particles a initial velocity is randomly sampled in the range between (v_x, v_y, v_z) and $(v_x+dv_x, v_y+dv_y, v_z+dv_z)$. The value of the distribution function in the elementary volume results from an average of the distribution function computed for all the test trajectories (existing and not existing).

- If the trajectory does not exist, the value of the distribution function is zero. A trajectory does not exist, when an environment population is tracked and if the initial position is on the spacecraft. In the inverse situation, a trajectory does not exist, when a secondary or a source population is tracked and if the initial position is on the environment.
- If the trajectory exists, the initial value of the distribution function is computed.

The backtracking technique implemented in SPIS is for the moment limited to the populations which are at about a stationary state and non collisional. When the characteristic time of electric field change is lower than the trajectory calculation time, a static electric field can not be considered. It would be possible to store the electric field at each time step to do a backward tracking of particles but it is too costly in memory. Thus it is not done in the present version of SPIS and a steady electric field is considered in the numerical particle detector instruments.

D. Phase space discretizarion

The backtracking algorithm quality is based essentially on the quality of the discretization of the velocity space. But most of the time the user can not estimate an accurate range for particle velocity detection, thus the velocity domain to backtrack is very large. To do an *a priori* discretization of the space velocity domain would imply to know approximately the distribution function results but it is not the case in general. The solution selected in SPIS is to use an adaptive meshing of the velocity space volume.

In order to adapt the mesh in course of the backtracking, an OcTree (see Fig. 10) technique is used to store the value of the

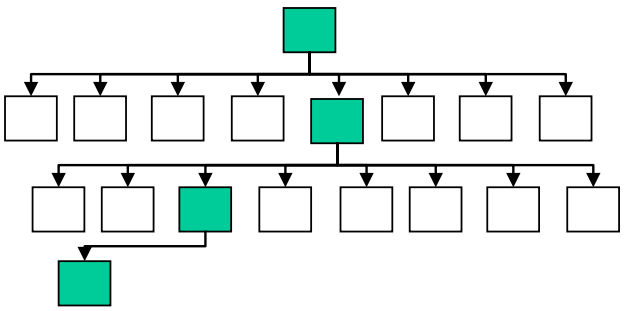

Fig. 10. OcTree architecture and the corresponding distribution function discretization in velocity space

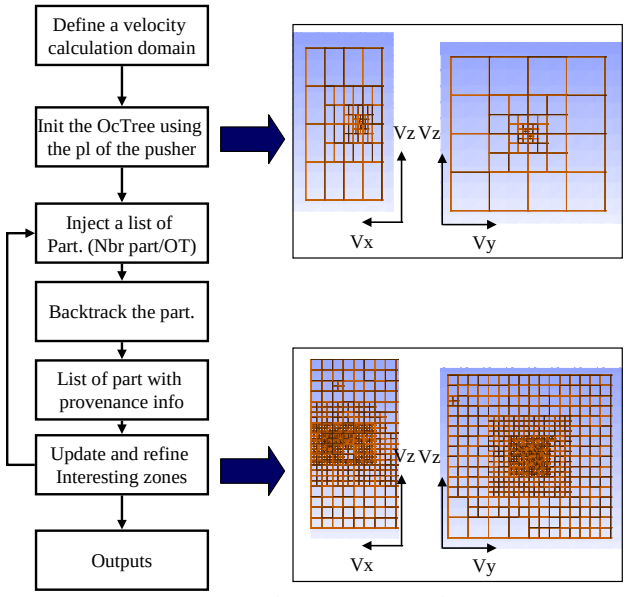

Fig. 11. Optimization heuristic for the distribution function discretization

distribution function. The principle of the OcTree algorithm is to start with a single slab representing the whole velocity space volume and then to successively split in eight sub-volumes (length divided by two in the three directions) the volumes you want to refine (as represented in the Fig. 11). This algorithm is in fact a dichotomy algorithm for splitting a mesh. Thus the convergence is very fast. The cell size is divided by 2^N in each direction with N the number of splitting. In 20 iterations, the precision of discretization in one direction can be $dv_x/10^6$.

The next step of the algorithm is thus to define what volumes element is interesting to split. In order to do this, an heuristic of optimization is defined. This heuristic is base on the fact two kinds of volume element are very interesting to improve:

- The volume elements where the distribution function value is the higher. In these volume elements of velocity, it is always interesting to increases the precision in order to increase the global precision of the calculation of the distribution function moments.
- The element where the test particles calculate very different distribution function. As the value is an average, it is interesting to split this volume to exactly compute for example the exact position of a distribution function gradient. An the inverse, if all the test particles of a volume elements computes the same value the distribution function, it is reasonable to think that it is not needed to refine this volume even if the value of the distribution function is the higher.
- The volume elements which have neighbors with a splitting level greater. This corresponds to a propagation of the splitting interest to neighbors (splitting diffusion).

It permits to have a very adaptable algorithm for the calculation of 3D distribution function of velocity on the detector. An auto-refinement technique with an heuristic approach is used to discretize the 3D distribution function

based on the OcTree techniques. It permits to capture a large range of distribution function from the smoother to the sharpest.

VI. Numerical method improvements

A. Statistics optimization

The particle statistics both volume and on surfaces is a challenge for any PIC code since the accuracy depends on the number of super-particles (SP) that can be reached on the simulation box. A first way to enhance the statistics consists in increasing the number of super particles injected at the simulation boundaries (external boundary or spacecraft). This is of course accompanied by an increase of the computational duration, proportional to that increase.

An advanced method based on local enhancement of the SP number injection is proposed. The lack of statistics on volume nodes is corrected by multiplying locally the number of SP injected. The statistics optimization consists first in gathering the information of the current location of particles with respect to their origin (from spacecraft surface or from the external boundary). A direct correspondence between volume statistics and surfaces of injection is obtained. Second, an algorithm increases the number of SP injected by boundary surfaces, focusing on particles able to reach regions of bad statistics.

In a near future, the same approach will be adopted to optimize the energy distribution of particles. It is thought to increase the statistics even better.

B. Performance Optimization

Several optimizations have been performed for gains of performance. First, the particle pusher has been improved by a multi-threading approach in which the particle list (up to millions of numerical super particles, each representing several real particles) is treated by different processors at the same time. The performance depends on the number of core that can be run in parallel. It is possible to reduce the cost of the particle pusher to the cost of other numerical modules, such as electric field and spacecraft surface potential calculation.

A second significant improvement has consisted in the modification of the spacecraft circuit solver. Indeed, a decrease of the performance was sometimes reported when large dielectrics surfaces on spacecraft were meshed with small grids. An iterative solver was developed and used instead of the previous exact Gauss method used to solve the linear system formed by the conductive, capacitive and inductive coupling of the spacecraft circuit. The Conjugate Gradient Squared (CGS) method permits to drastically reduce the cost (by a factor 3 at least).

Lastly, a new monitor has been developed to provide the computational cost (CPU cost) of each part of the code including the calculation of: particle transport, electric field, spacecraft circuit, results generation. A summary is provided at the end of the simulation (more frequent outputs can be generated), which gives the user information on which processes impact the duration of the simulation.

VII. Conclusions

This paper presented the new SPIS 5 version capabilities in term of advanced numerical modelling of plasma spacecraft interactions. The detailed approach has been presented for the most important components and a discussion of the limitations of these approaches. A validation campaign of the SPIS 5 numerical core has been done and is presented in different companion papers.

Acknowledgment

This work was supported by ESA "SPIS-SCIENCE" contract no. 4000102091/10/NL/AF and "SPIS-GEO" contract no. 4000101174/10/NL/AF. The authors want to acknowledge A. Eriksson, C. Cully and T. Nilsson from IRFU for their help during the user requirements phase and the organization of the 17th SPINE meeting at Uppsala in 2011. The authors would also thanks all the active participants of the SPINE community for the inputs on the requirements.

References

[1] J. Roussel, F. Rogier, G. Dufour, J.-C. Mateo-Velez, J. Forest, A. Hilgers, D. Rodgers, L. Girard, and D. Payan, "SPIS open-source code: Methods, capabilities, achievements, and prospects," *Plasma Sci. IEEE Trans. On*, vol. 36, no. 5, pp. 2360–2368, 2008.

[2] J. Roussel, F. Rogier, G. Dufour, J.-C. Mateo-Velez, J. Forest, A. Hilgers, D. Rodgers, L. Girard, and D. Payan, "SPIS Open-Source Code: Methods, Capabilities, Achievements, and Prospects," *IEEE Trans. Plasma Sci.*, vol. 36, no. 5, pp. 2360–2368, Oct. 2008.

[3] J. Roussel, G. Dufour, J.-C. Mateo-Velez, B. Thiebault, B. Andersson, D. Rodgers, A. Hilgers, and D. Payan, "SPIS Multitimescale and Multiphysics Capabilities: Development and Application to GEO Charging and Flashover Modeling," *IEEE Trans. Plasma Sci.*, vol. 40, no. 2, pp. 183–191, 2012.

[4] "Spis website: http://dev.spis.org/."

[5] A. Hilgers, B. Thiebault, D. Estublier, E. Gengembre, J. A. Gonzalez Del Amo, M. Capacci, J.-F. Roussel, M. Tajmar, and J. Forest, "A Simple Model of the Effect of Solar Array Orientation on SMART-1 Floating Potential," *IEEE Trans. Plasma Sci.*, vol. 34, no. 5, pp. 2159–2165, Oct. 2006.

[6] J. Berthelier, J. Yang, J. Forest, and M. Quassim, "DEMETER potential measurements: Observations from the ion analyzer, model calculation using SPIS and implications for plasma and field measurements," in *Proc. 10th Spacecraft Charging Technol. Conf*, pp. 18–21.

[7] A. I. Eriksson, E. Engwall, R. Prakash, L. Daldorff, R. Torbert, I. Dandouras, and K. Torkar, "Making use of spacecraft–plasma interactions: Determining tenuous plasma winds from wake observations and numerical simulations," in *Proceedings of the 10th Spacecraft Charging Technology Conference*, 2007.

[8] J.-C. Mateo-Velez, J. Roussel, D. Sarrail, F. Boulay, V. Inguimbert, and D. Payan, "Ground Plasma Tank Modeling and Comparison to Measurements," *IEEE Trans. Plasma Sci.*, vol. 36, no. 5, pp. 2369–2377, 2008.

[9] J.-C. Mateo-Velez, J. Roussel, V. Inguimbert, M. Cho, K. Saito, and D. Payan, "SPIS and MUSCAT Software Comparison on LEO-Like Environment," *IEEE Trans. Plasma Sci.*, vol. 40, no. 2, pp. 177–182, 2012.

[10] A. Hilgers, S. Clucas, B. Thiebault, J.-F. Roussel, J.-C. Mateo-Velez, J. Forest, and D. Rodgers, "Modeling of Plasma Probe Interactions With a PIC Code Using an Unstructured Mesh," *IEEE Trans. Plasma Sci.*, vol. 36, no. 5, pp. 2319–2323, Oct. 2008.

[11] J.-C. Mateo-Velez, J.-F. Roussel, T. Tondu, F. Boulay, D. Sarrail, and E. Chesta, "Neutralization for Micro Propulsion - Experiments and SPIS Simulations," 2008.

[12] D. Rodgers, S. Clucas, and D. Nicolini, "SPIS simulations in optimization of FEEP design and contamination analysis," in

Proceedings of 11th Spacecraft Charging Tech. Conf.,, Albuquerque, NM, USA, 2010.

[13] J.-F. Roussel, T. Tondu, J.-C. Mateo-Velez, E. Chesta, S. D'Escrivan, and L. Perraud, "Modeling of FEEP Plume Effects on MICROSCOPE Spacecraft," *IEEE Trans. Plasma Sci.*, vol. 36, no. 5, pp. 2378–2386, Oct. 2008.

[14] P. Sarrailh, J.-F. Rousse, J.-M. Siguier, V. Inguimbert, G. Murat, and J. SanMartin, "LEO Drifting Plasma Collection by a Positive Biased Tether Wire: Time/-Dependant Simulations using SPIS," in *Proceedings of 12th Spacecraft Charging Technology Conf.*, Kitakyushu, Japan, 2012.

[15] S. Guillemant, V. Génot, J.-C. Matéo-Vélez, R. Ergun, and P. Louarn, "Solar wind plasma interaction with solar probe plus spacecraft," in *Annales Geophysicae*, 2012, vol. 30, pp. 1075–1092.

[16] S. Guillemant, V. Genot, J.-C. M. Velez, P. Sarrailh, A. Hilgers, and P. Louarn, "Simulation Study of Spacecraft Electrostatic Sheath Changes With the Heliocentric Distances from 0.044 to 1 AU," *IEEE Trans. Plasma Sci.*, vol. Early Access Online, 2013.

[17] S. Guillemant, V. Génot, J.-C. Matéo-Vélez, R. Ergun, and P. Louarn, "Solar wind plasma interaction with solar probe plus spacecraft.," *Ann. Geophys. 09927689*, vol. 30, no. 7, 2012.

[18] "SPINE website: http://dev.spis.org/projects/spine/home/meeting/mxvii."

[19] F. Rogier, J.-F. Roussel, and D. Volpert, "Approximations filaires pour les équations de Poisson et de Maxwell harmoniques," *Comptes Rendus Math.*, vol. 343, no. 10, pp. 633–636, Nov. 2006.

SPIS 5: new modelling capabilities and method for scientific mission

Spacecraft Charging Technology Conference, 23-27 June, 2014, Pasadena, California, USA

P. Sarrailh, J.-C. Matéo-Vélez, S. Hess, J.-F. Roussel (1)
B. Thiébault, J. Forest, B. Jeanty-Ruard, (2)
A. Hilgers, D. Rodgers, F. Cipriani (3)

(2) ARTENUM, PARIS Science & Groupware

(1) ONERA THE FRENCH AEROSPACE LAB

(3) esa

Outline

- Introduction
  - Zoom on most recent activities
  - Spine community
  - SPIS general overview
- Modelling improvements illustration:
  - Global precision
  - Virtual instruments
  - Unmeshed elements: wire and thin panels
  - Semi transparent grids
- Conclusion & Perspectives

Zoom on most recent activities

SPIS-GEO

- ESTEC/ESA contract
- Technical officer: David Rodgers
- Consortium: Artenum, ONERA, EADS-Astrium, OHB-Sweden

- Adaptation to industrial needs, in particular to GEO/MEO
  - Industrial user needs
  - Simplified user interface adapted to engineering applications
  - Physical models adaptated to GEO/MEO
  - Tested software against in-flight observations and existing codes

- Finalized in March 2013
- Maintenance phase closed in September 2013

SPIS-SCIENCE

- ESTEC/ESA contract
- Technical officer: Alain Hilgers
- Consortium: ONERA, Artenum, IRF-U, IRAP

- Long-term scientific program of ESA : missions dealing with plasma measurements (Solar Orbiter, Juice)
- SPIS new capabilities
  - Electrostatic cleanliness assessment
  - SPIS adapted to relatively low energy (few eV) plasma measurements with a large number of physical models implemented
  - Tested on Solar Orbiter (particle instruments), Cluster (particle & electric field), Rosetta (electric field) and Cassini (electric field)

- Finalized in November 2013
- Maintenance phase till September 2014

esa

ONERA
THE FRENCH AEROSPACE LAB

ARTENUM, PARIS
Science & Groupware

Software improvements

- SPIS 5 solvers improvements since the SPIS 4 version :
  - Precision
  - Performance
  - User-defined ambient plasma and spacecraft interactions
  - Pre-defined transient phases
  - Instruments → How to mimic scientific particle detectors, Langmuir probes, electric field analyzers
  - Unmeshed elements

- New stable version of the software → SPIS v. 5.1.2 (available on SPIS website)
  - Open Source and freely available on SPIS website (http://dev.spis.org)
  - Includes SPIS-GEO, SPIS-SCIENCE and some elements from AISEPS (EP)
  - Bug fixes from the SPIS v. 5.1.0 RC

- SPINE, an active community
  - Regular SPINE meetings and training courses → inputs for SPIS development program / exchange between SPIS users
  - Active forum
  - Numerous publications

SPIS simulation principle

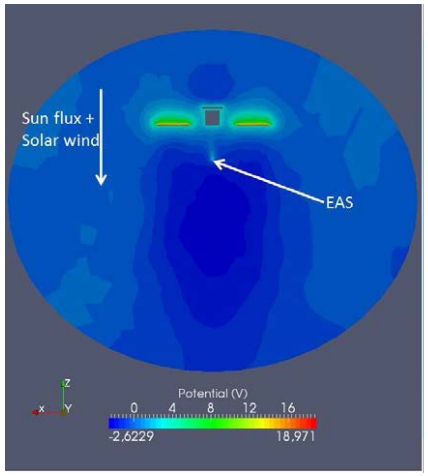

courtesy Stanislas Guillemant (IRAP, ONERA)

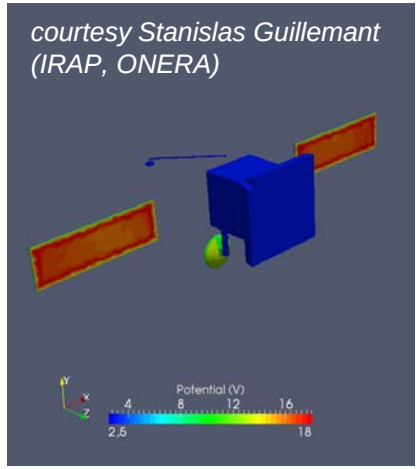

① Electric field from:
-Particle densities
-Boundary conditions

④ Potential on S/C:
-Current balance
-RLC circuit between S/C elements

② Particle Transport:
-Space environment
-Secondaries or Sources from S/C

③ Interaction with S/C:
-SEE by electrons
-SEE by protons
-Photo-emission
-Sources

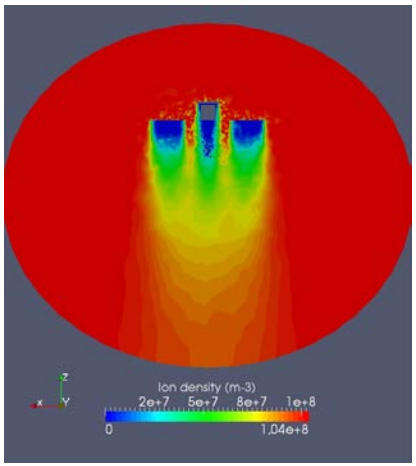

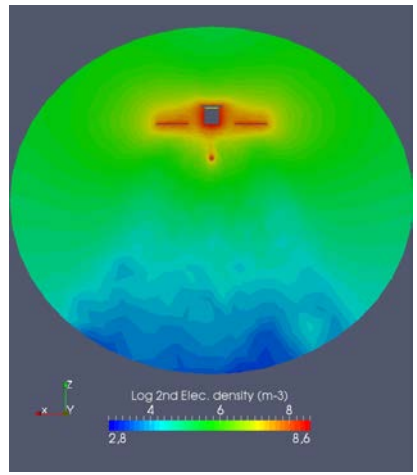

Software improvements

- Global precision improvements
  - Injection at the environment boundary conditions
  - User define and not limited number of environment population
  - Pusher method in presence of magnetic field
  - Optimization method for injection
- Performance:
  - UI to NUM refactoring
  - Multi thread pusher
- Instruments:
  - Particle detector
  - Virtual probes
  - Langmuir probes
- Unmeshed elements
  - Thin wire modeling with a very small radius in comparison to the mesh size (booms, antena, RPW instrument,…)
  - Thin panels modeling with a very small thickness in comparison to the mesh size (solar array for example)
  - SA interconnectors modeling with a very small size in comparison to the mesh size
  - Virtual instrument not interacting with the simulation
  - Semi-Transparent Grid (STG) without meshing the aperture

Software improvements

- **Global precision improvements**
  - **Injection at the environment boundary conditions**
  - **User define and not limited number of environment population**
  - Pusher method in presence of magnetic field
  - Optimization method for injection
- **Performance:**
  - **UI to NUM refactoring**
  - **Multi thread pusher**
- Instruments:
  - Particle detector
  - Virtual probes
  - Langmuir probes
- Unmeshed elements
  - Thin wire modeling with a very small radius in comparison to the mesh size (booms, antena, RPW instrument,…)
  - Thin panels modeling with a very small thickness in comparison to the mesh size (solar array for example)
  - SA interconnectors modeling with a very small size in comparison to the mesh size
  - Virtual instrument not interacting with the simulation
  - Semi-Transparent Grid (STG) without meshing the aperture

esa ONERA THE FRENCH AEROSPACE LAB ARTENUM, PARIS Science & Groupware

Global precision improvements

Characteristics of a spherical probe immersed in maxwellian plasma

Quantity	Value (a)	Value (b)
Temperature	0.5 eV	0.2 eV
Electron/ion density	6.91×10^{8} m^{-3}	2.763×10^{10} m^{-3}
Debye length	0.2 m	0.02 m
Potential	[0 to 12.5 V]	[0 to 5 V]
Sphere radius	0.1 m	0.02 m
Particle model	full-PIC	full-PIC
Number of tetrahedrons	127,759	56,726
Simulation box diameter	1.3 m	0.2 m
Number of macro-particles	430,000 to 1,500,000	193,000 to 650,000

SPIS 4 error ~3-5 %

SPIS 5 error < 1%

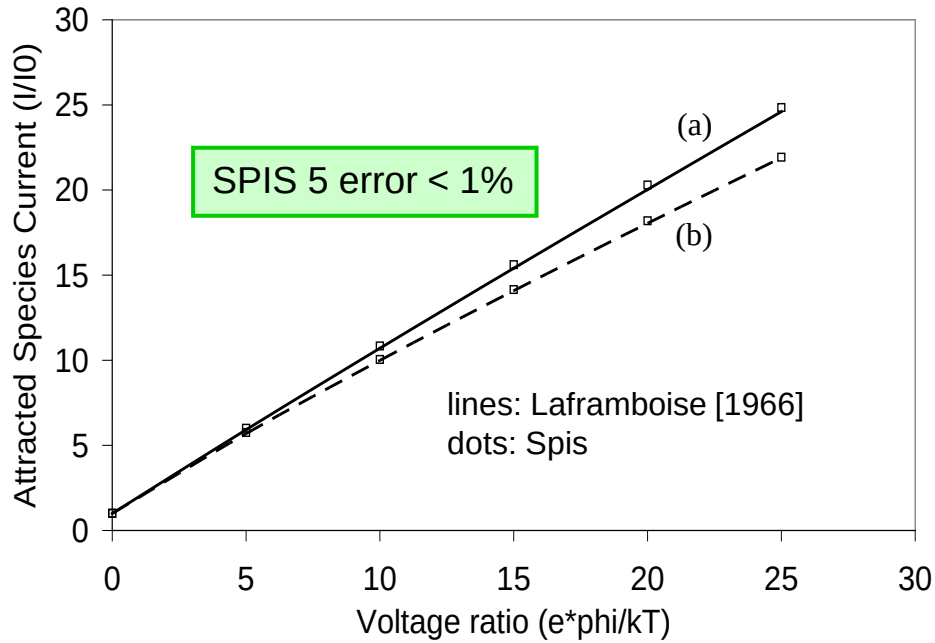

esa

ONERA
THE FRENCH AEROSPACE LAB

ARTENUM, PARIS
Science & Groupware

Global precision improvements

Characteristics of a cylindrical probe immersed in maxwellian plasma

SPIS 4 error > 10 %

Quantity	Value
Temperature	0.2 eV
Electron/ion density	2.76×10^{10} m^{-3}
Debye length	0.02 m
Potential	[0-5 V]
Cylinder radius	0.02 m
Cylinder length	0.08 m
Number of tetrahedrons	45,000
Simulation box diameter	0.4 m
Number of macro-particles	460,000

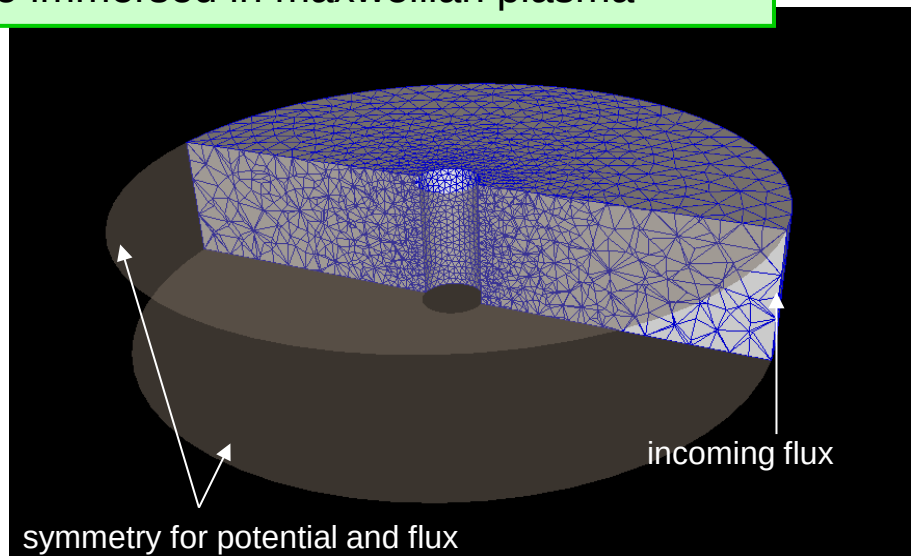

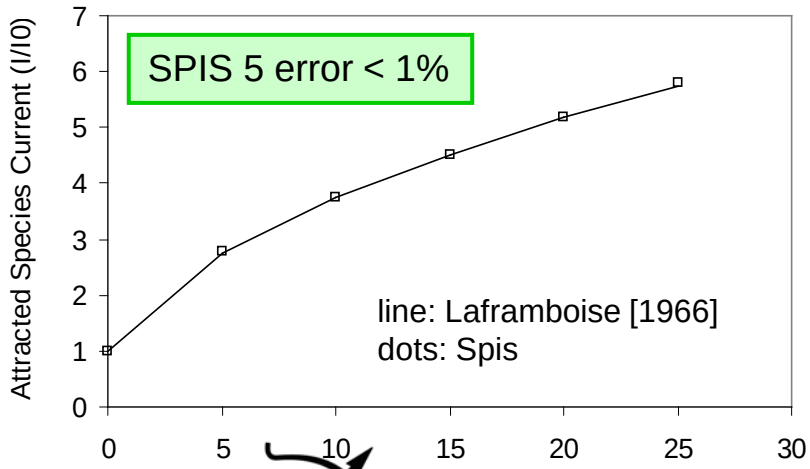

Software improvements

- Global precision improvements
  - Injection at the environment boundary conditions
  - User define and not limited number of environment population
  - Pusher method in presence of magnetic field
  - Optimization method for injection
- Performance:
  - UI to NUM refactoring
  - Multi thread pusher
- **Instruments:**
  - **Particle detector**
  - Virtual probes
  - Langmuir probes
- **Unmeshed elements**
  - **Thin wire modeling with a very small radius in comparison to the mesh size (booms, antena, RPW instrument,…)**
  - Thin panels modeling with a very small thickness in comparison to the mesh size (solar array for example)
  - SA interconnectors modeling with a very small size in comparison to the mesh size
  - Virtual instrument not interacting with the simulation
  - Semi-Transparent Grid (STG) without meshing the aperture

esa

ONERA
THE FRENCH AEROSPACE LAB

ARTENUM, PARIS
Science & Groupware

Onboard instrument problematic

- Solar Orbiter mission:
  - Three-axis stabilized spacecraft, Sun pointing
  - Solar wind plasma
  - Closest Sun encounter 0.28 AU (2017 launch)
  - Validation case performed in collaboration between ONERA/IRAP (**S. Guillemant, J.-C. Matéo-Velez, V. Génot and P. Sarrailh**)

Sun Flux (#1AU)	12,76
Electrons Ne (m-3) / Te (eV)	$1{,}04 \times 10^8$ / 21,37
Ions H+ Ni (m-3) / Ti (eV)	$1{,}04 \times 10^8$ / 27,00
Vz ram H+ (km/s) / Mach Number	400 / 7,86
Debye length (m)	3,38
Debye length photoelec (m)	0,27

- Modelling problematic:
  - Computation of the electron velocity distribution function as measured by EAS
  - Particles from environment influenced by SC charge and space charge in volume
  - Contamination of secondary populations
  - Multi-scale problematic → typical length scale:

  Detector aperture << potential variation

  (1 mm) << (~ 10 m)

- Method used:
  - 1st step: standard SPIS simulation
  - 2nd step: "backtracking"

  from the detector to compute the EVDF

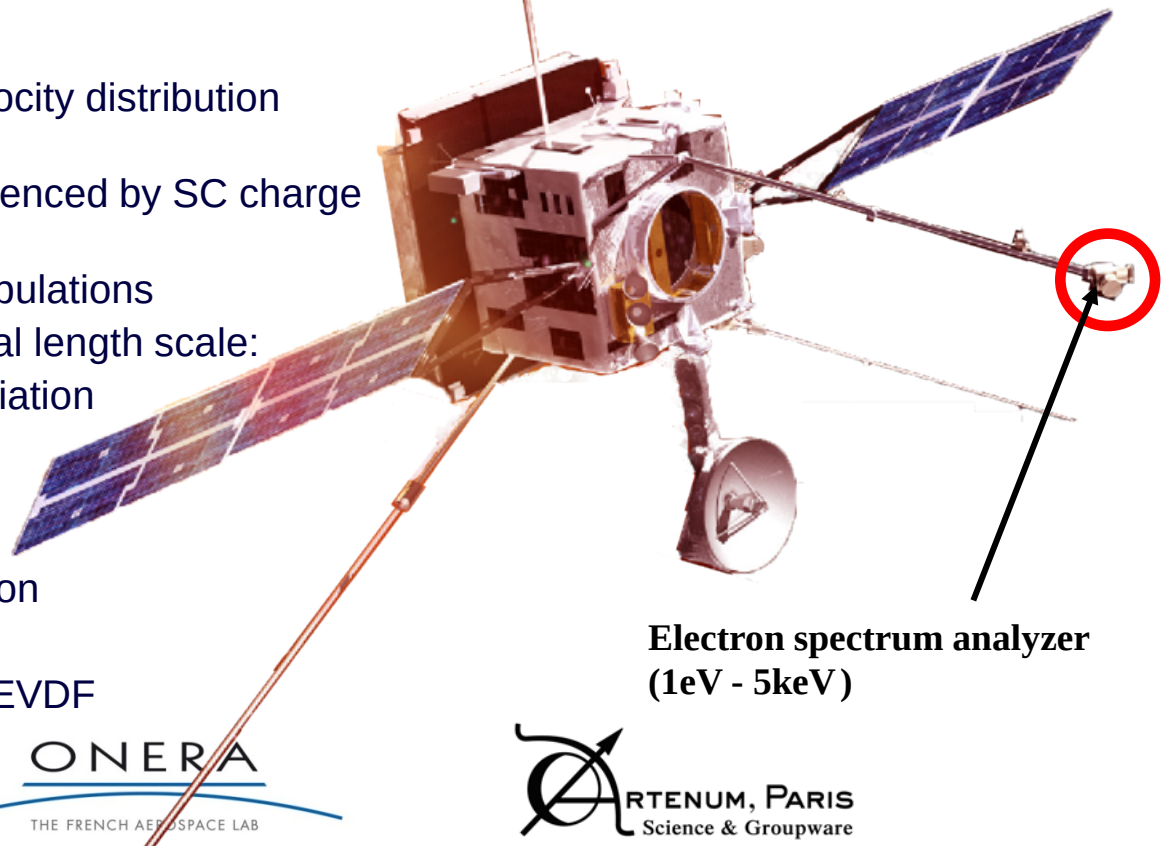

Electron spectrum analyzer (1eV - 5keV)

1st step: standard SPIS simulation

- Electrons : e- with Particle in Cell (PIC) modeling
- Ions : H+ with Particle in Cell (PIC) modeling
- Photoelectrons: PIC modeling of a Maxwellian distribution, Temperature = 3 eV
- Secondary electrons: PIC modeling of a Maxwellian distribution, Temperature 2 eV, backscattered electrons simulated (with 2/3 of their initial energy)
- External boundary conditions : Fourier, $1/R^2$ decrease of potential
- No magnetic field considered

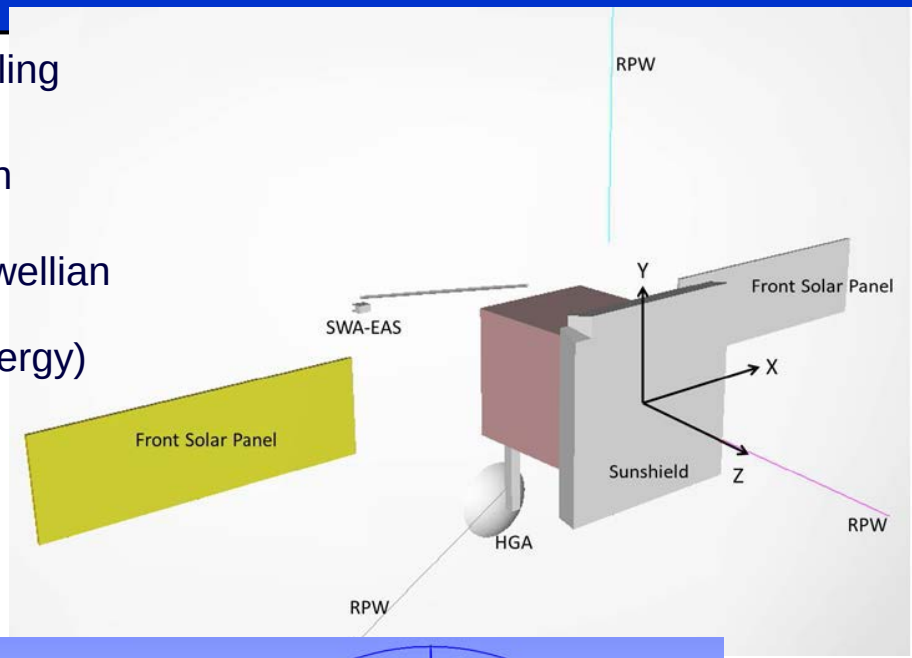

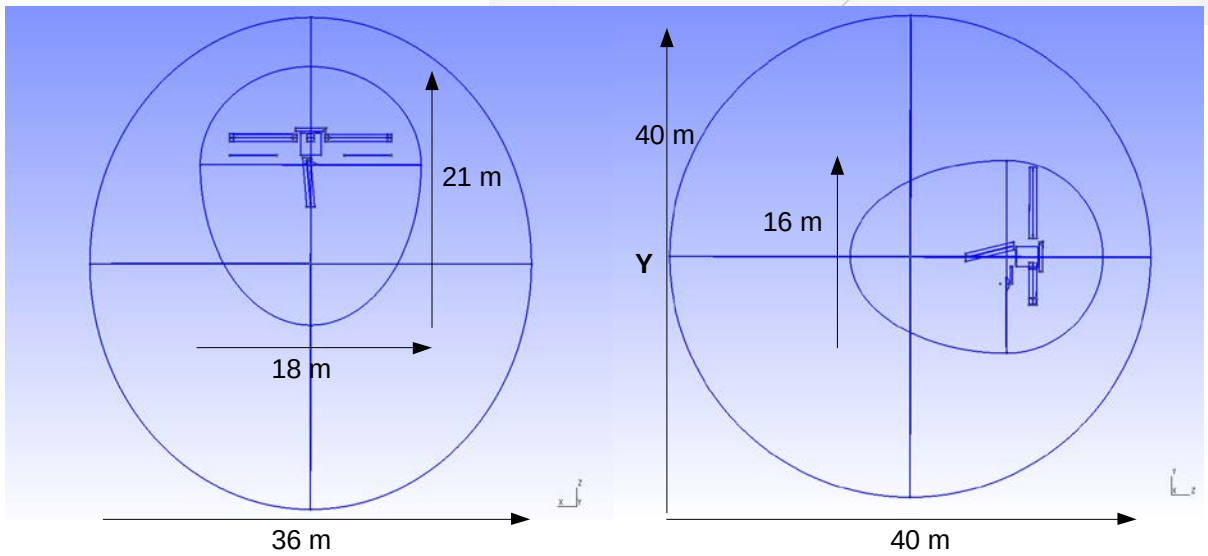

Principle of "Backtracking"

- Main objective:
  - Compute the 3V distribution function in velocity on an arbitrary surface in the computation domain
  - Control the result statistic on the surface

➢ Algorithm details:

★ Based on Liouville theorem:

- ➢ Conservation of the space phase volume along a trajectory
- ➢ Existence or not of the trajectory from the detector surface
- ➢ Distribution function on the boundary conditions
- ➢ E and B fields are stationary // time scale of particle transport

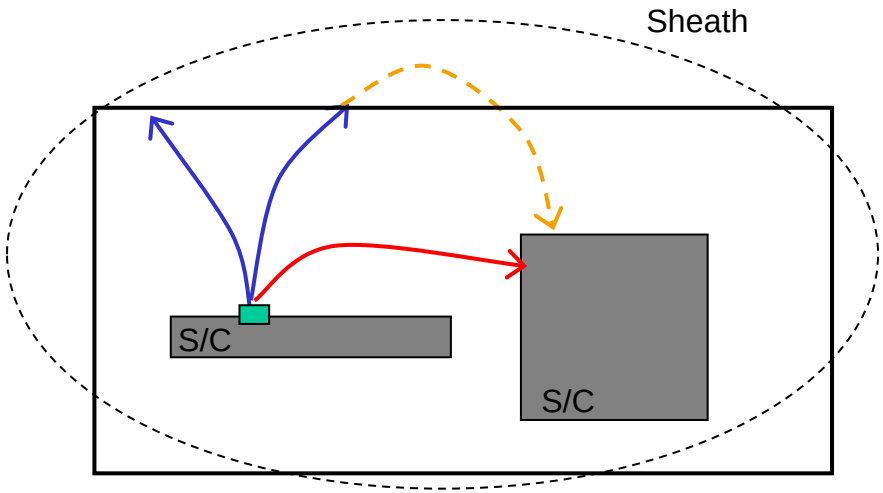

Simulation box boundary

$$\left(\vec{x}_B, \vec{\mathrm{v}}_\mathrm{B}\right) \xrightarrow{Traj} \left(\vec{x}_D, \vec{\mathrm{v}}_\mathrm{D}\right)$$

$$f_D\left(\vec{x}_D, \vec{\mathrm{v}}_\mathrm{D}, t\right) = f_B\left(\vec{x}_B, \vec{\mathrm{v}}_\mathrm{B}, t\right)$$

★ Key point: discretization of the phase space DF

- ➢ Use of an OcTree algorithm (adaptive refinement of the phase space DF)
- ➢ Use of the forward tracking particles to initiate the OcTree
- ➢ Heuristic for discretization adaptation based on the reduction of the statistical error on the momentums of the DF and on the dispersion of events

esa ONERA THE FRENCH AEROSPACE LAB ARTENUM, PARIS Science & Groupware

Adaptive algorithm based on OcTree

- Algorithm based on OcTree:

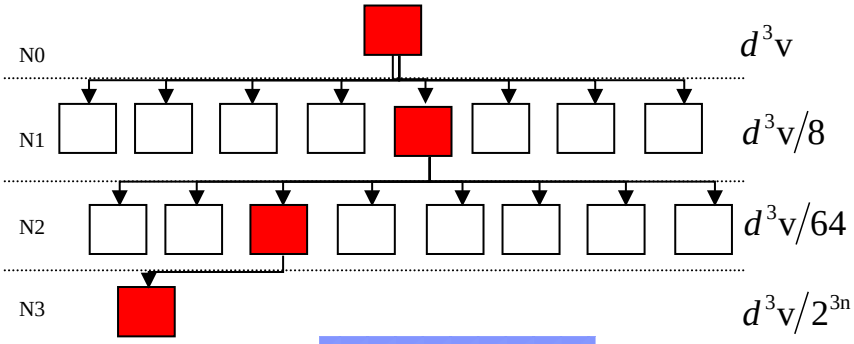

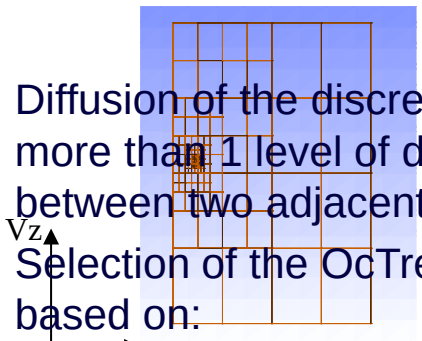

→ Diffusion of the discretization: no more than 1 level of difference between two adjacent OcTrees

→ Selection of the OcTree to split based on:

1. Convergence of the first momentum ($f.d^3v$)
2. Statistic variation on the DF inside one OcTree: $|\langle f^2 \rangle - \langle f \rangle^2|$

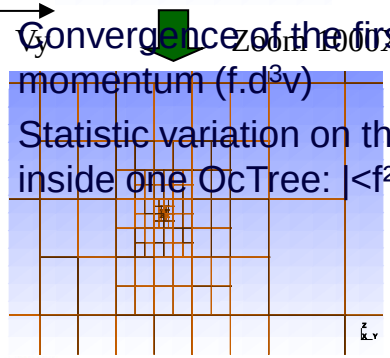

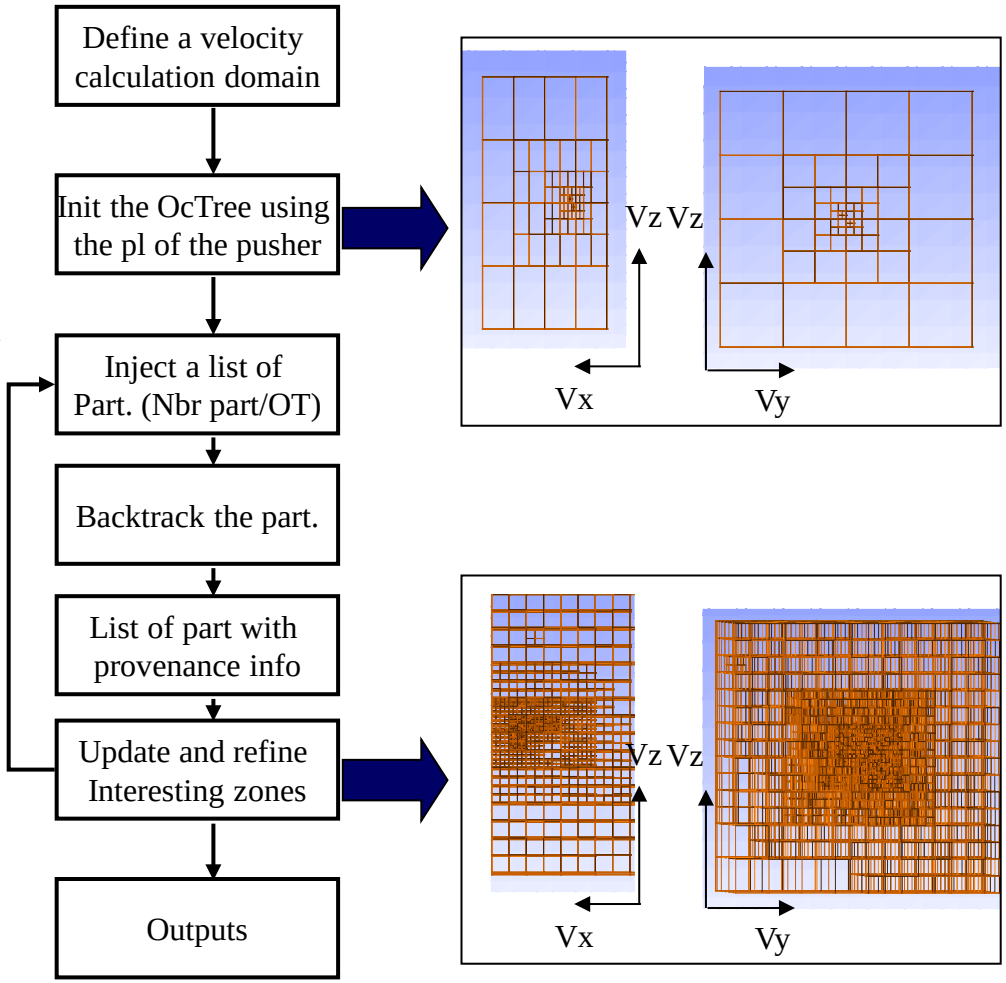

esa

ONERA
THE FRENCH AEROSPACE LAB

ARTENUM, PARIS
Science & Groupware

Solar wind electron detection

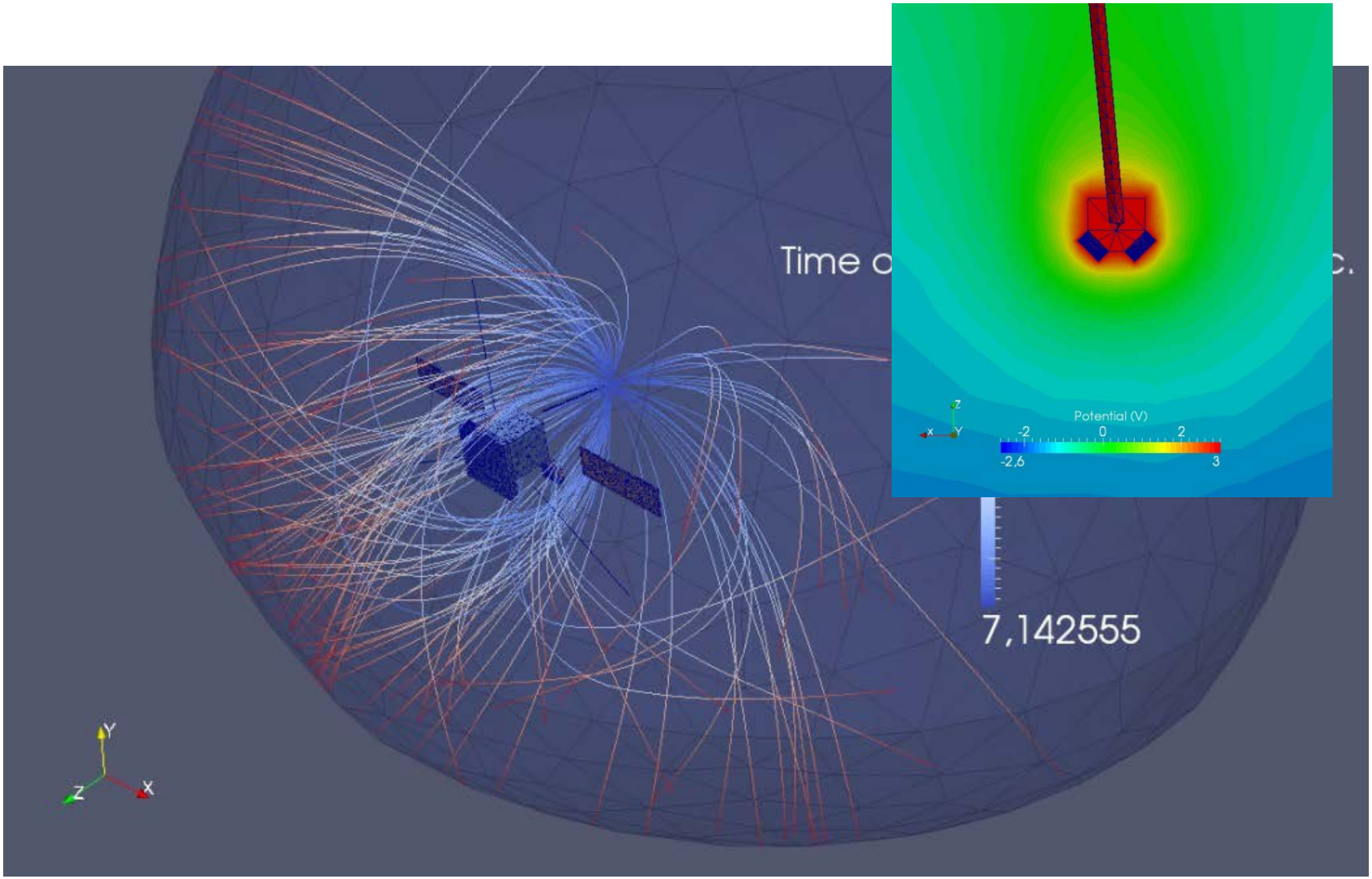

Photo electron detection

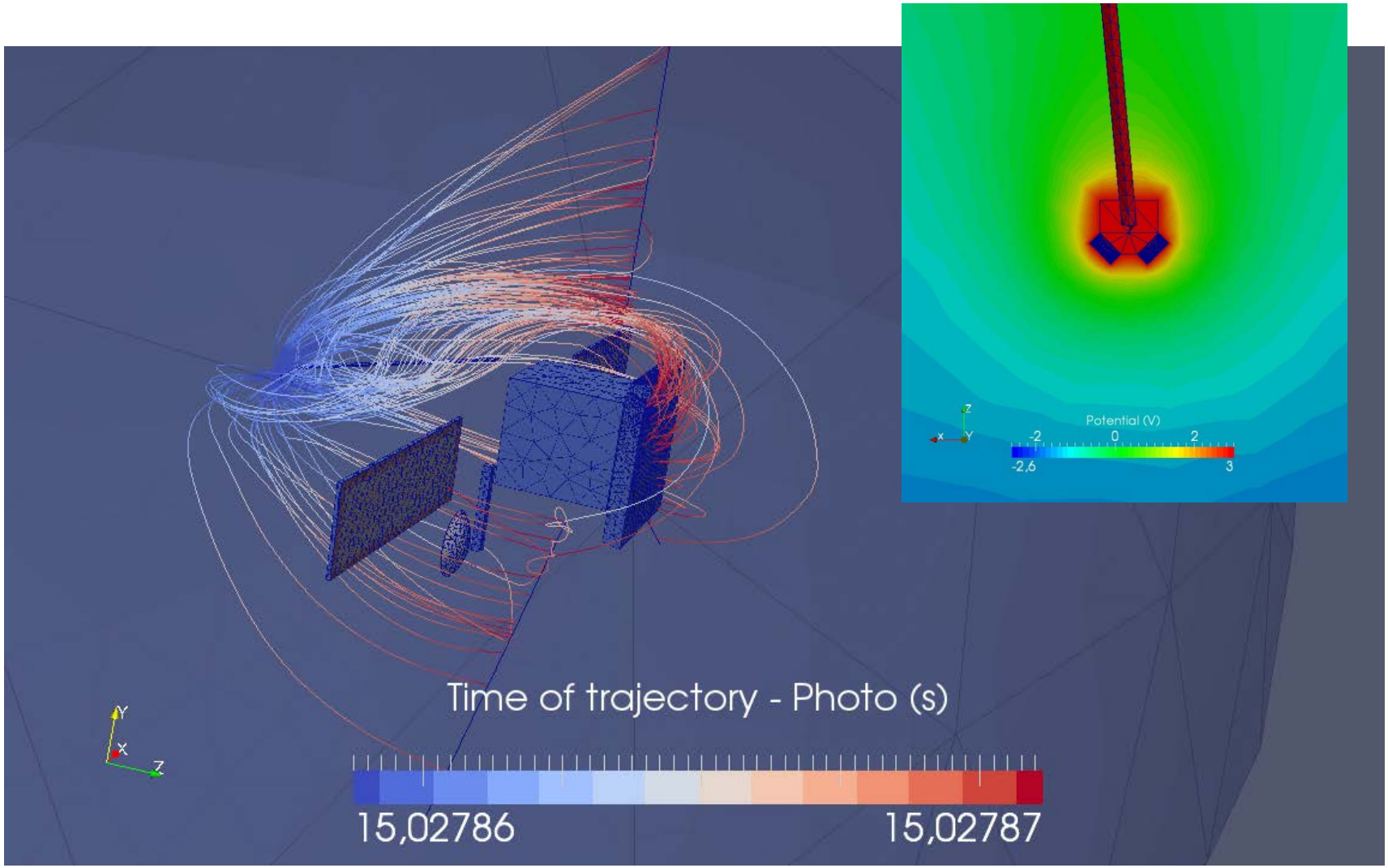

Secondary electron from electron impact

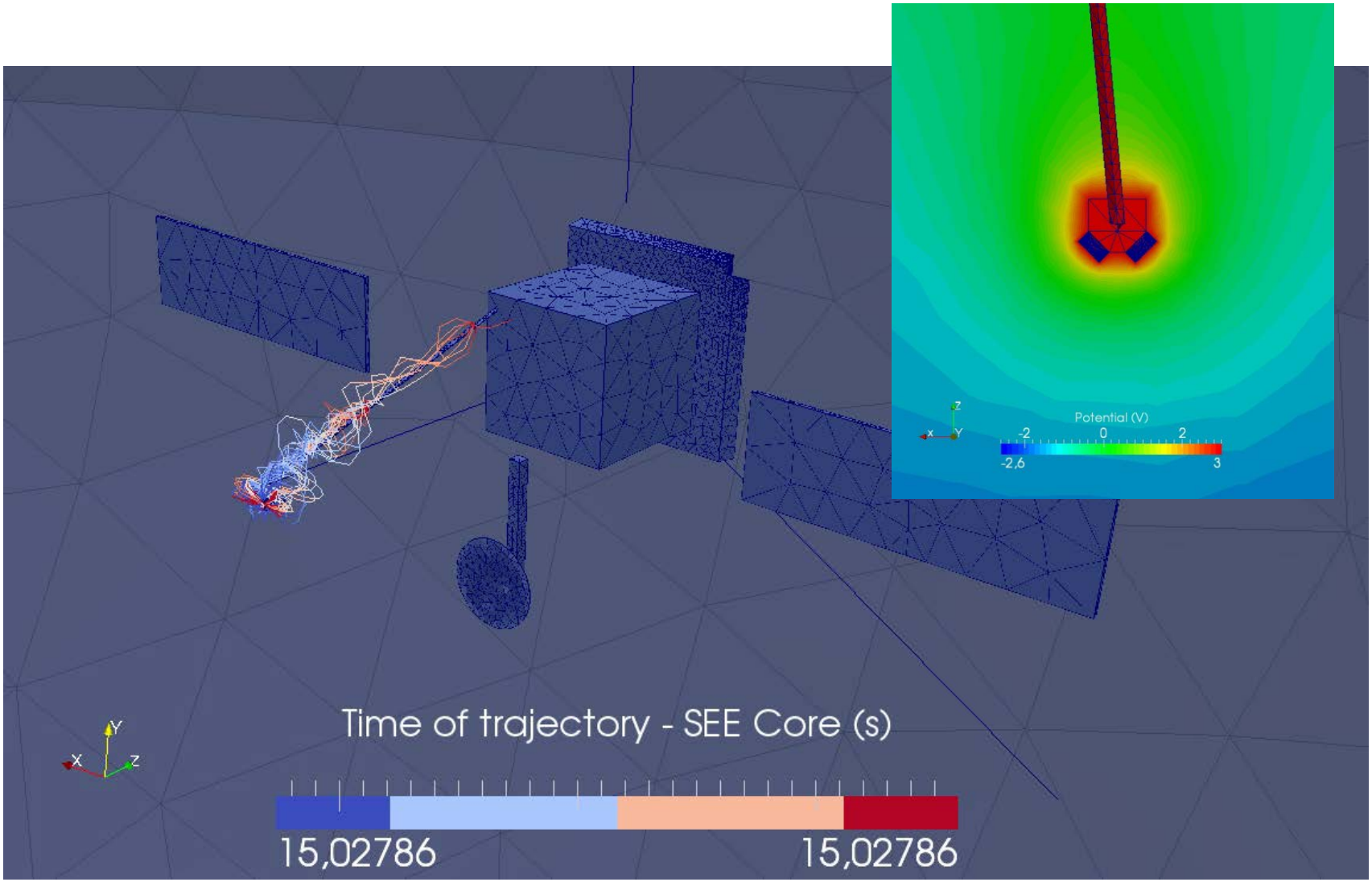

Particle Detectors – Example of DF results

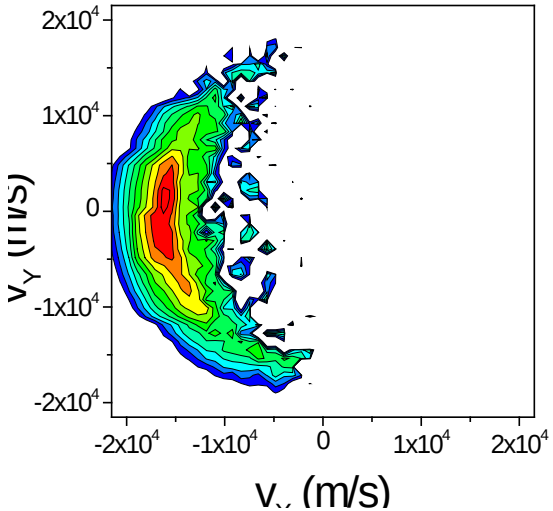

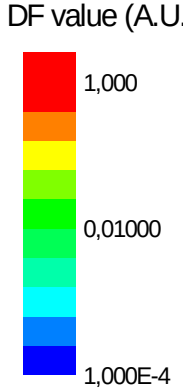

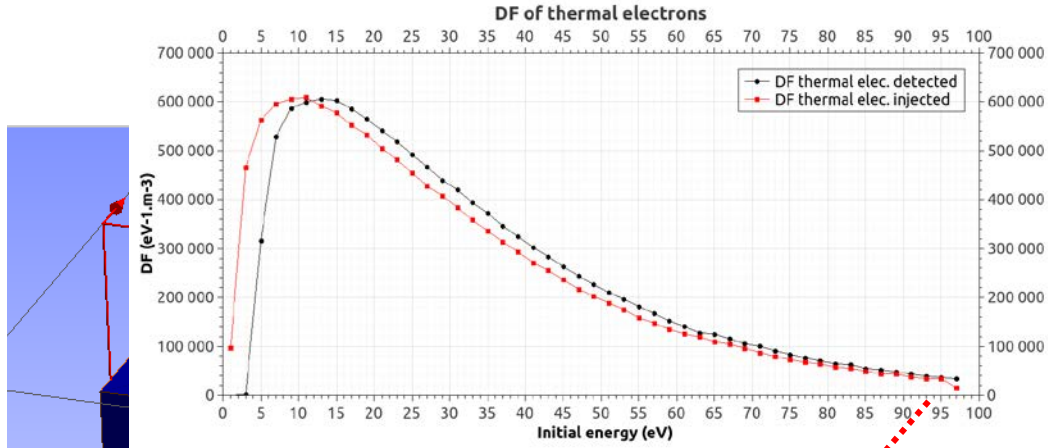

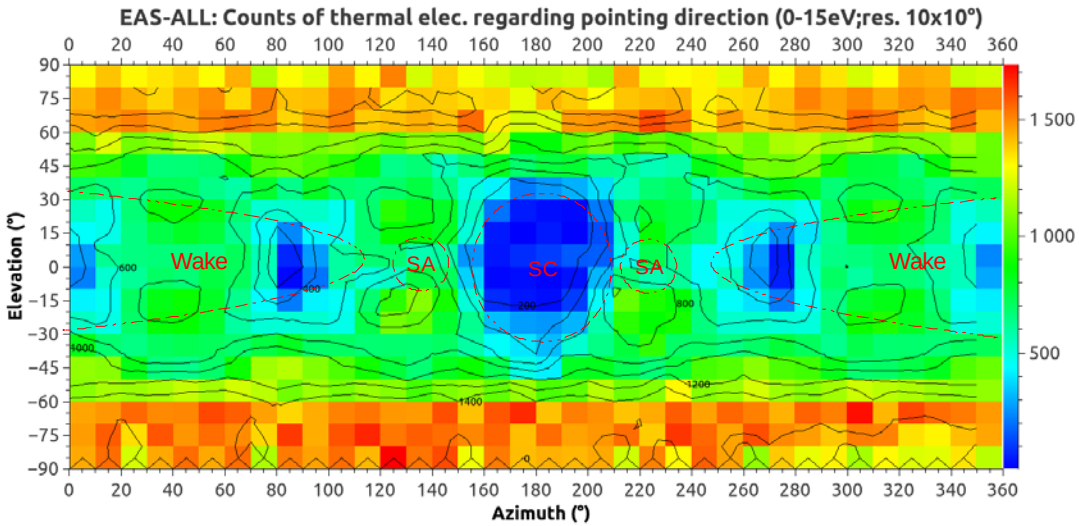

Software improvements

- Global precision improvements
  - Injection at the environment boundary conditions
  - User define and not limited number of environment population
  - Pusher method in presence of magnetic field
  - Optimization method for injection
- **Performance:**
  - **UI to NUM refactoring**
  - **Multi thread pusher**
- Instruments:
  - Particle detector
  - Virtual probes
  - Langmuir probes
- **Unmeshed elements**
  - **Thin wire modeling with a very small radius in comparison to the mesh size (booms, antena, RPW instrument,…)**
  - **Thin panels modeling with a very small thickness in comparison to the mesh size (solar array for example)**
  - **SA interconnectors modeling with a very small size in comparison to the mesh size**
  - Virtual instrument not interacting with the simulation
  - Semi-Transparent Grid (STG) without meshing the aperture

esa

ONERA
THE FRENCH AEROSPACE LAB

ARTENUM, PARIS
Science & Groupware

Unmeshed elements – Thin wires/Thin Panels

- Thin elements in SPIS:
  - 1D → thin wires (booms, antenna, …)
    when r << Δx
  - 2D → thin panels (solar panels, …)
    when h << Δx
- One or two dimensions not meshed (respectively radius and thickness)
- but take into account:
  - Potential calculation (wire singularity or panel edges singularity)
  - Current collection (wire radius)
  - Current emission (surface area, impinging angle for SEE, …)

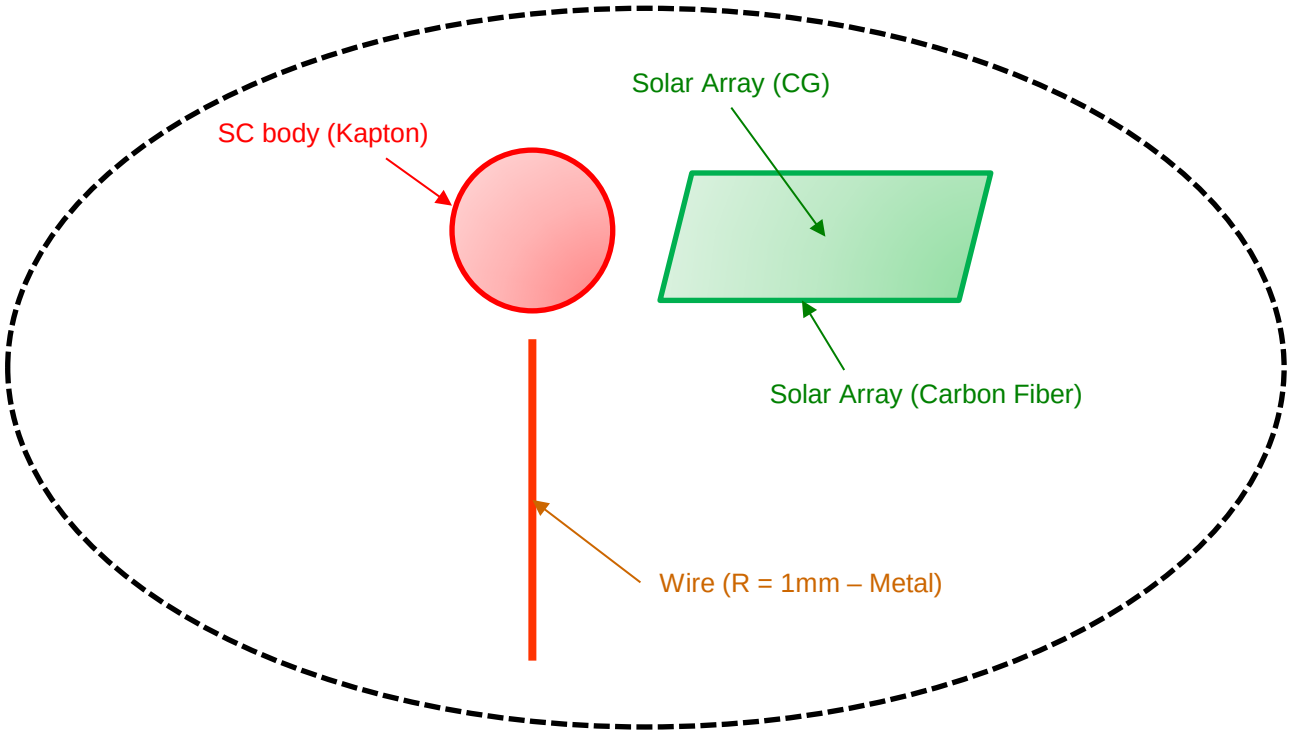

Solar Array 4m x 2m:
- Mesh size Δx = 0.2 m
- SA thickness h = 0.05 m

Too costly to mesh h → without 2D thin elements Δx < h/2 !!!

Wire 4m:
- Mesh size Δ x = 0.2 m
- Radius R = 1 mm

Too costly to mesh r → without 1D thin elements Δx < r/2 !!!

Unmeshed elements – Thin wires/Thin Panels

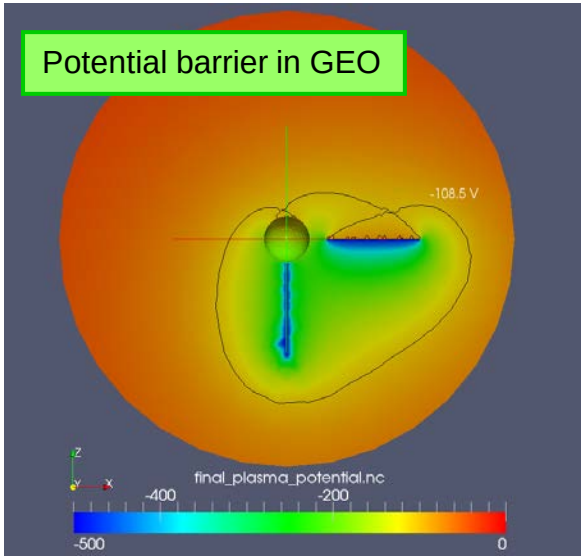

- Potential map:
  - Smooth potential jump → good description of the potential barrier
  - Potential effect of the wire
- Emission and collection:
  - On the wire → small effect because small radius
  - On the thin panel → standard surface (face A dielectric and face B conductor)
- Shading effect of the SC on the wire
- Wire → intensivelly used in the validation cases

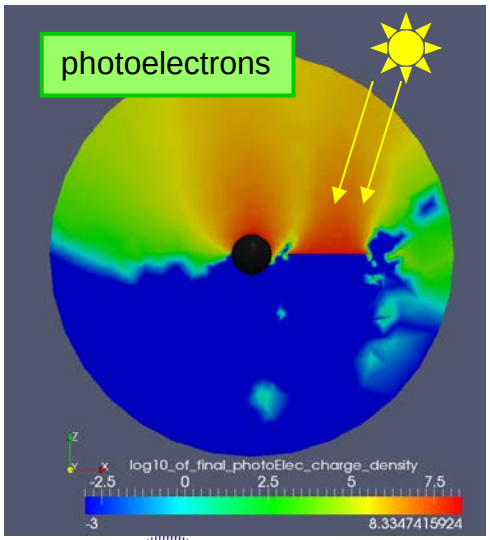

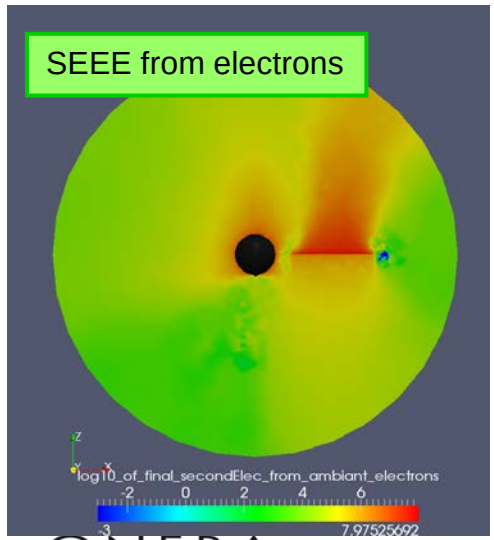

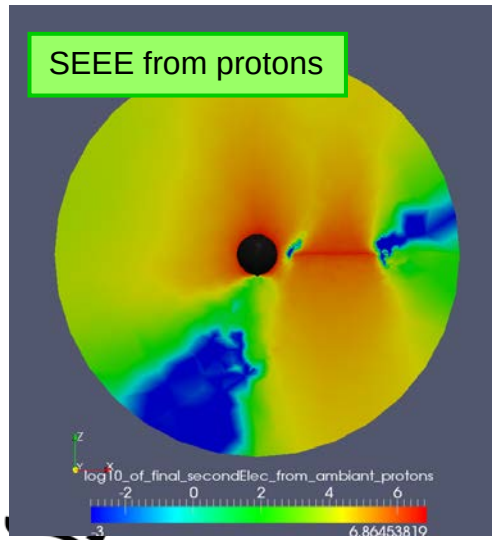

Software improvements

- Global precision improvements
  - Injection at the environment boundary conditions
  - User define and not limited number of environment population
  - Pusher method in presence of magnetic field
  - Optimization method for injection
- **Performance:**
  - **UI to NUM refactoring**
  - **Multi thread pusher**
- Instruments:
  - Particle detector
  - Virtual probes
  - Langmuir probes
- Unmeshed elements
  - Thin wire modeling with a very small radius in comparison to the mesh size (booms, antena, RPW instrument,…)
  - Thin panels modeling with a very small thickness in comparison to the mesh size (solar array for example)
  - SA interconnectors modeling with a very small size in comparison to the mesh size
  - Virtual instrument not interacting with the simulation
  - **Semi-Transparent Grid (STG) without meshing the aperture**

Unmeshed elements – Semi-Transparent Grids (STG)

- Aperture not meshed → transparency coefficient
- Functionnal test sequence #2 (simplified RPA)

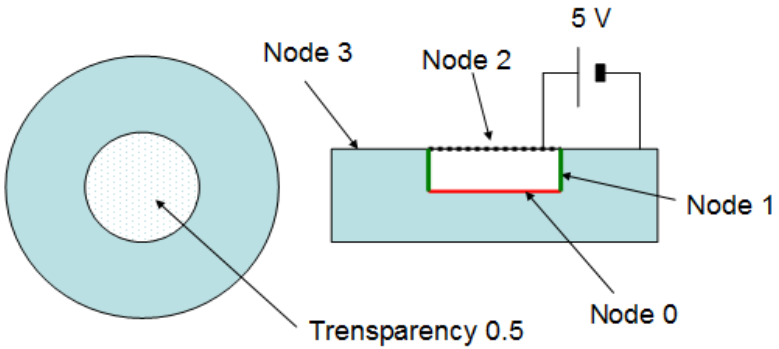

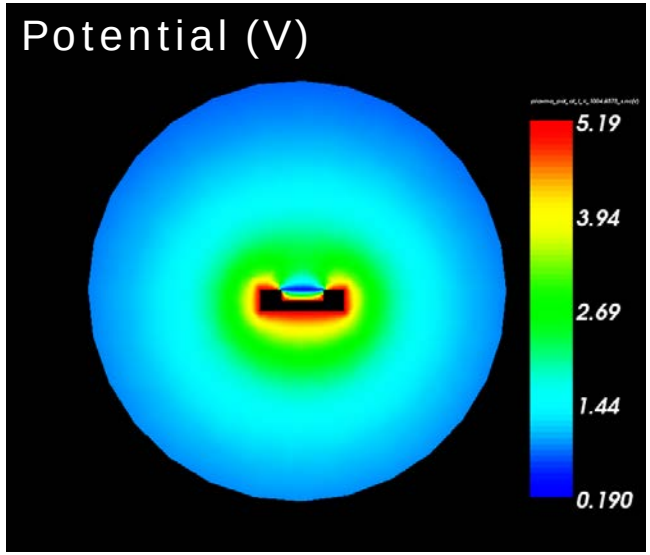

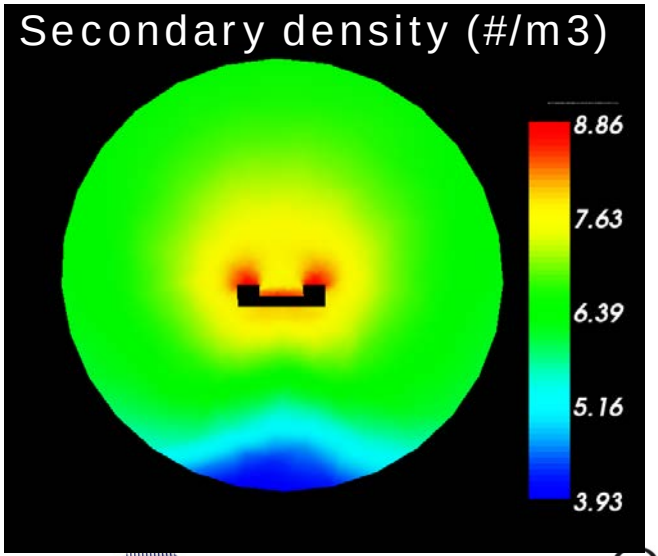

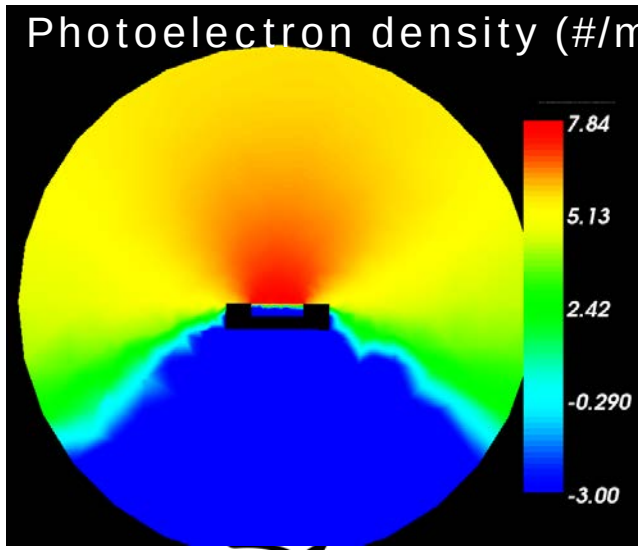

Repulsive Electron Potential Analyzer – REPA

- Measurement of the surface voltage of a material during continuous electron irradiation in CEDRE facility
- Grid analyser system based on the attraction or repulsion of the secondary electrons

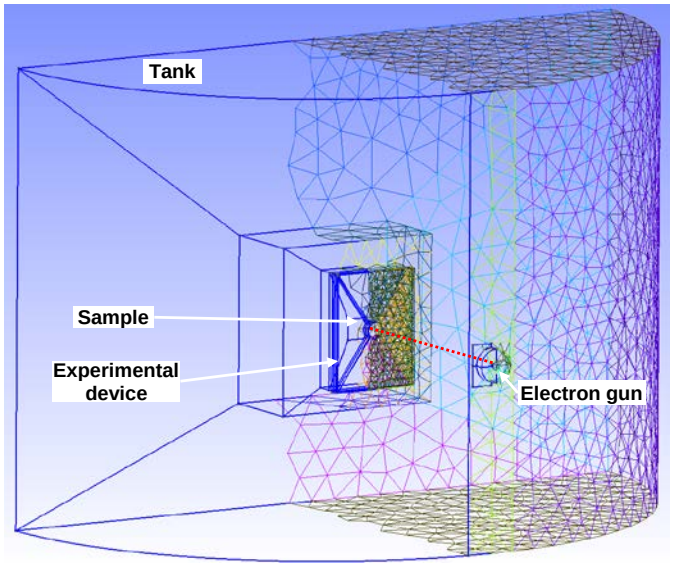

- Paper by K. Guerch to be published

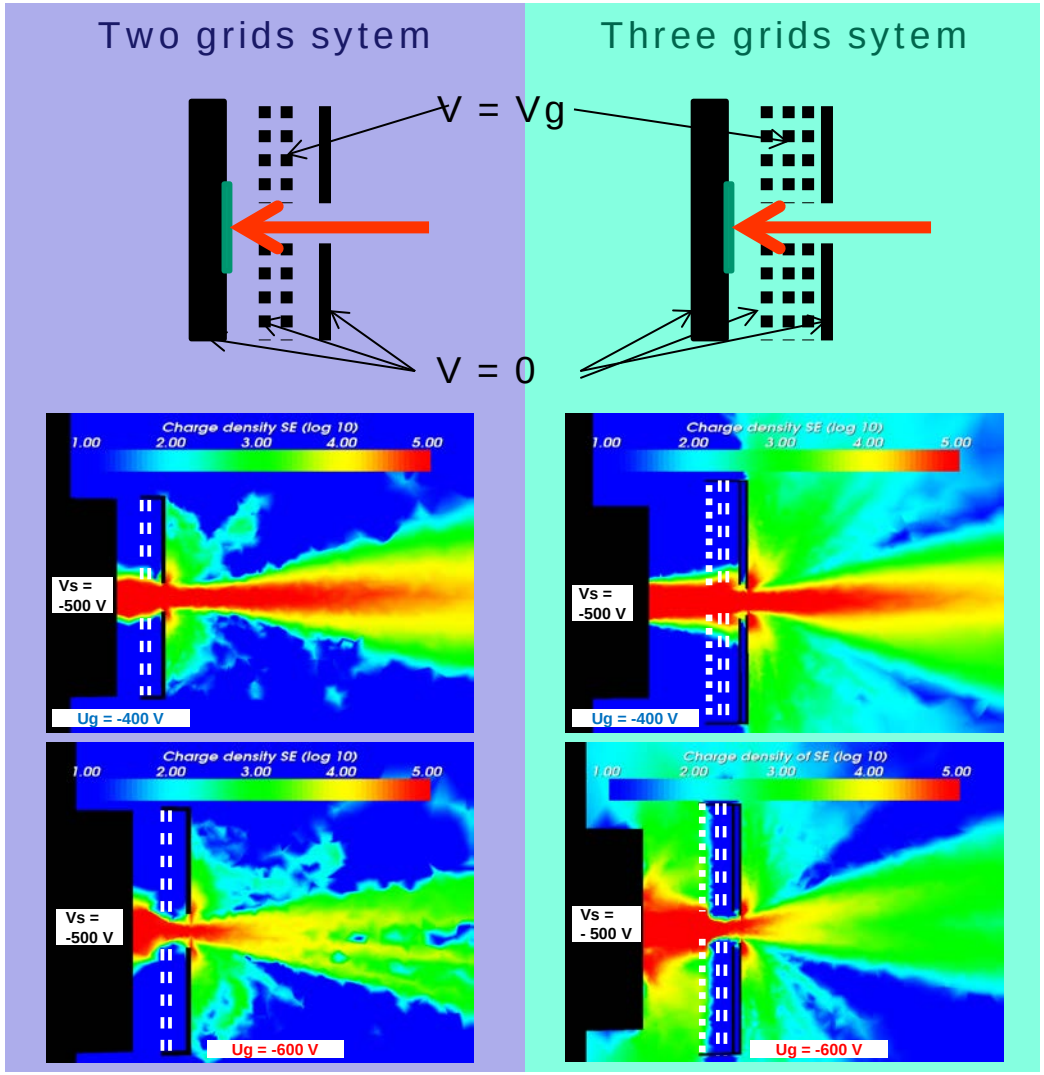

Conclusion

- Set of newly developed modules tested and validated for GEO and SCIENCE applications
  - User-friendly interface
  - Advanced physical modelling
- Lot's of practical cases for scientific applications, GEO applications and on ground modelling
- Software and set of test and validation cases available in SPIS 5.1 from GEO and SCIENCE project
- Application/Validation cases, comparison with other software and experiments available in SCTC papers:
  - Study and Simulation of Low Energy Plasma Measurement on Solar Orbiter (S. Guilleman, Onera)
  - GEO spacecraft worst-case charging estimation by numerical simulation (J.-C. Mateo-Velez, Onera)
  - Simulation and analysis of spacecraft charging using SPIS-GEO and NASCAP-GEO (B. Theillaumas, Airbus-DS)
  - Surface Charging of the Jupiter Icy Moons Explorer (JUICE) (F. Cipriani, ESA)
  - Extension of SPIS to simulate dust electrostatic charging, transport and contamination of lunar probes (P. Sarrailh, Onera)

esa

ONERA
THE FRENCH AEROSPACE LAB

ARTENUM, PARIS
Science & Groupware